AMERICAN MUSEUM NOVITATES

Number 4038, 40 pp. June 19, 2025

A Multigene Phylogeny for *Oecomys* (Rodentia: Cricetidae: Sigmodontinae) with Descriptions of New and Revalidated Taxa and a Partial Species-Group Classification

ROBERT S. VOSS,[1] THOMAS C. GIARLA,[2] BURTON K. LIM,[3] AND MARK D. ENGSTROM[4]

ABSTRACT

We report phylogenetic analyses of a multigene dataset for 24 species of the Neotropical cricetid genus *Oecomys*, including one new species from western Amazonia (*O. hiceae*) and a revalidated trans-Andean species (*O. trabeatus*). In addition, we analyze sequence data from four species that have not previously been included in any molecular analysis (*O. flavicans*, *O. phaeotis*, *O. speciosus*, and *O. trinitatis* sensu stricto) and from historical specimens of *O. concolor* (a species represented in previous analyses by sequences of problematic homology). Our results provide strong support for a monophyletic Rutilus Group (including *O. hiceae*, *O. rutilus*, *O. trabeatus*), a Bicolor Group (*O. bicolor*, *O. cleberi*, *O. nanus*, *O. jamari*, *O. phaeotis*), and a Mamorae Group (*O. franciscorum*, *O. mamorae*). We tentatively recognize two other clades that are less strongly supported by our analytic results but that seem to merit heuristic recognition: a Concolor Group (*O. concolor, O. speciosus*) and a Trinitatis Group (*O. catherinae*, *O. flavicans*, *O. matogrossensis*, *O. rex*, *O. trinitatis*). Future taxonomic progress will require sequence data from additional genes, revisionary studies of still problematic species (e.g., *O. bicolor*, *O. trinitatis*), and fresh collections from hitherto poorly surveyed regions.

[1] Department of Mammalogy, American Museum of Natural History.
[2] Department of Biology, Siena College, Loudonville, NY.
[3] Department of Mammalogy, Royal Ontario Museum, Toronto, ON, Canada.
[4] Department of Mammalogy, Royal Ontario Museum, Toronto, ON, Canada.

 ISSN 0003-0082

INTRODUCTION

Members of the genus *Oecomys* Thomas, 1906, are semiarboreal cricetids of the sigmodontine tribe Oryzomyini that occur in rainforests and dry forests from Costa Rica to northern Argentina. Formerly ranked as a subgenus of *Oryzomys* Baird, 1857, *Oecomys* was once believed to contain only two species (Hershkovitz, 1960), but subsequent revisionary research has shown that it is among the most speciose oryzomyine genera (Carleton and Musser, 2015; Pardiñas et al., 2016; Saldanha and Rossi, 2021; Saldanha et al., 2023; Voss et al., 2024). Twenty-two species are currently recognized as valid (table 1), but several are believed to represent species complexes (Rocha et al., 2018; Suárez-Villota et al., 2018; Silva et al., 2020, 2022), and additional taxa remain to be described or resurrected from synonymy.

One impediment for efficient progress toward a taxonomic revision of *Oecomys* is the absence of a robustly supported phylogeny and a meaningful species-group classification. Although some phylogenetic structure is apparent in recent analyses of molecular sequence data (e.g., Suárez-Villota et al., 2018; Voss et al., 2024), no analysis to date has included genetic data from all currently recognized species, some species are represented only by mitochondrial sequences, and multispecies clades identified by previous analyses have yet to be diagnosed morphologically. Although we are currently unable to rectify all these problems, the multigene dataset analyzed in this report is a step in the right direction.

Herein we compile sequence data from the mitochondrial gene encoding cytochrome *b* (CYTB) and from two nuclear loci: exon 1 of the gene encoding interphotoreceptor retinoid-binding protein (IRBP) and intron 7 of the gene encoding beta fibrinogen (FGB). We obtained sequence data from at least one gene for exemplars of all currently recognized species, four of which—*Oecomys flavicans*, *O. phaeotis*, *O. speciosus*, and *O. trinitatis* (sensu stricto)—have not previously been included in any molecular analysis.

Additionally, we analyze sequence data from western Amazonian specimens previously identified as *Oecomys paricola* by Carleton and Musser (2015). Cytochrome *b* sequences from this material are strikingly divergent from those of topotypical (eastern Amazonian) specimens of *O. paricola*. This report documents morphological differences and molecular comparisons that, together with our phylogenetic results, justify recognition of a new western Amazonian species.

Lastly, we analyze sequence data from specimens of *Oecomys trabeatus*, a trans-Andean taxon previously synonymized with *O. bicolor*. Sequence data from *O. trabeatus* suggest that it is not closely related to *O. bicolor*, from which it also differs morphologically. We redescribe *O. trabeatus* as a valid species herein.

MATERIALS AND METHODS

Voucher material: The specimens examined for this report and others represented by sequence data that we downloaded from GenBank are in the following collections (listed in order of their traditional abbreviation): AMNH (American Museum of Natural History, New York), ANSP (Academy of Natural Sciences of Drexel University, Philadelphia), BMNH (Natural History Museum, London), CM (Carnegie Museum of Natural History, Pittsburg), FMNH

TABLE 1. Currently recognized species of *Oecomys* (not including taxa revalidated or described as new in this report).

	Distribution[a]
O. auyantepui Tate, 1939	Guiana Region (NE Amazonia)
O. bicolor (Tomes, 1860)	Amazonia, Central America, and W Ecuador
O. catherinae Thomas, 1909	SE Amazonia, Cerrado, and Atlantic Forest[b]
O. cleberi Locks, 1981	Cerrado[c]
O. concolor (Wagner, 1845)	Rio Negro and upper Río Orinoco basins
O. flavicans (Thomas, 1894)	N Venezuela and N Colombia
O. franciscorum Pardiñas et al., 2016	Chaco of N Argentina[d]
O. galvez Voss et al., 2024	W Brazil, E Ecuador, and NE Peru[e]
O. jamari Saldanha et al., 2023	W Brazil (Rondônia)[f]
O. makampi Voss et al., 2024	NE Peru[e]
O. mamorae (Thomas, 1906)	E Bolivia, NW Paraguay[g]
O. matogrossensis Saldanha and Rossi, 2021	Mato Grosso, SW Pará, and Rondônia (Brazil)[h]
O. nanus Voss et al., 2024	W Brazil, NE Peru[e]
O. paricola (Thomas, 1904)	SE Amazonia[i]
O. phaeotis (Thomas 1901)	NE Bolivia and SE Peru
O. rex Thomas, 1910	Guiana Region (NE Amazonia)
O. roberti (Thomas, 1904)	Amazonia (widespread)
O. rutilus Anthony, 1921	Guiana Region (NE Amazonia)
O. speciosus (Allen and Chapman, 1893)	Trinidad, N Venezuela, and NE Colombia
O. superans Thomas, 1911	W Amazonia
O. sydandersoni Carleton et al., 2009	NE Bolivia
O. trinitatis (Allen and Chapman, 1893)	Trinidad and NE Venezuela[j]

[a] As mapped by Carleton and Musser (2015) except as noted.
[b] Distribution of the "*Oecomys catherinae* species group" sensu Suárez-Villota et al. (2018).
[c] Brandão et al. (2024).
[d] Pardiñas et al. (2016).
[e] Voss et al. (2024).
[f] Saldanha et al. (2023).
[g] Records of this species mapped by Carleton and Musser (2015) from E Paraguay and Mato Grosso do Sul (Brazil) are possibly based on specimens of *O. franciscorum*.
[h] Saldanha and Rossi (2021).
[i] As restricted in this report.
[j] As restricted by Voss et al. (2024: 78). Carleton and Musser's (2015) concept of this species included material collected throughout Amazonia and in eastern Central America).

(Field Museum of Natural History, Chicago), INPA (Instituto Nacional de Pesquisas da Amazônia, Manaus), KU (University of Kansas Biodiversity Research Center, Lawrence), MCZ (Museum of Comparative Zoology, Harvard University, Cambridge), MHNLS (Museo de Historia Natural La Salle, Caracas), MN (Museu Nacional, Universidade Federal do Rio de Janeiro, Rio de Janeiro), MSB (Museum of Southwestern Biology, University of New Mexico, Albuquerque), MUSM (Museo de Historia Natural de la Universidad Nacional Mayor de San Marcos,

Lima), MVZ (Museum of Vertebrate Zoology, University of California, Berkeley), MZUSP (Museu de Zoologia da Universidade de São Paulo, São Paulo), ROM (Royal Ontario Museum, Toronto), TTU (Museum of Texas Tech University, Lubbock), UFES (Universidade Federal do Espírito Santo, Vitória), UFROM (Coleção de Mamíferos da Universidade Federal de Rondônia, Porto Velho), UMMZ (University of Michigan Museum of Zoology, Ann Arbor), and USNM (National Museum of Natural History, Washington DC).

Morphological characters and descriptive conventions: The morphological terminology used in this report follows Weksler (2006), who illustrated and described most taxonomically relevant features of oryzomyine external and craniodental morphology. However, illustrations of preputial gland morphology—not illustrated by Weksler (2006) —are in Voss and Linzey (1981). Except as noted, the new and revalidated species described herein conform to the morphological diagnosis of *Oecomys* provided by Carleton and Musser (2015); therefore, only characters useful for distinguishing congeneric taxa are mentioned.

Measurements: Except as noted, external measurements are those taken in the field by collectors using the standard American protocol (Hall, 1962, 1980). We transcribed total length (nose to fleshy tail-tip, TL) and length of tail (basal flexure to fleshy tip, LT) from specimen labels or field notes, and we computed head-and-body length (HBL) by subtracting LT from TL. We also transcribed length of hind foot (heel to tip of longest claw, HF), length of ear (from notch, Ear), and weight from specimen labels or field notes, but we sometimes remeasured HF on skins and fluid-preserved specimens to check the accuracy of values recorded by collectors, and we used our values whenever discrepancies were found. We measured middorsal fur length and length of the terminal caudal hairs with a plastic ruler. All external measurements are reported to the nearest millimeter (mm), and all weights are reported to the nearest gram (g).

We measured skulls and teeth with digital calipers to the nearest 0.01 mm, and we used unrounded values to compute descriptive statistics and statistical tests, but measurements and statistics reported in our tables and text are rounded to the nearest 0.1 mm (the smallest decimal fraction of a millimeter that is consistently obtainable with repeated caliper measurements). The following dimensions were measured (fig. 1): CIL, condyloincisive length (from the greater curvature of one upper incisor to the articular surface of the ipsilateral occipital condyle); LD, length of diastema (from the lesser curvature of an upper incisor to the crown of the ipsilateral first upper molar); LM, length of molars (greatest crown length of the upper molar row); BM1, breadth of M1 (greatest transverse dimension of the crown of either the left or right first upper molar); LIF, length of incisive foramen (greatest anterior-posterior dimension of either the left or right incisive foramen); BIF, breadth of incisive foramina (greatest transverse dimension across both foramina); BPB, breadth of palatal bridge (breadth of the palate between the crowns of the right and left first upper molars); BZP, breadth of the zygomatic plate (least width of the zygomatic plate from its anterior to posterior margins); LIB, least interorbital breadth (the least transverse dimension between the orbits across the frontal bones); ZB, zygomatic breadth (the greatest transverse dimension across the zygomatic arches); LR, length of rostrum (distance from the distal apex of an intact nasal bone to the posterior margin of the ipsilateral zygomatic notch).

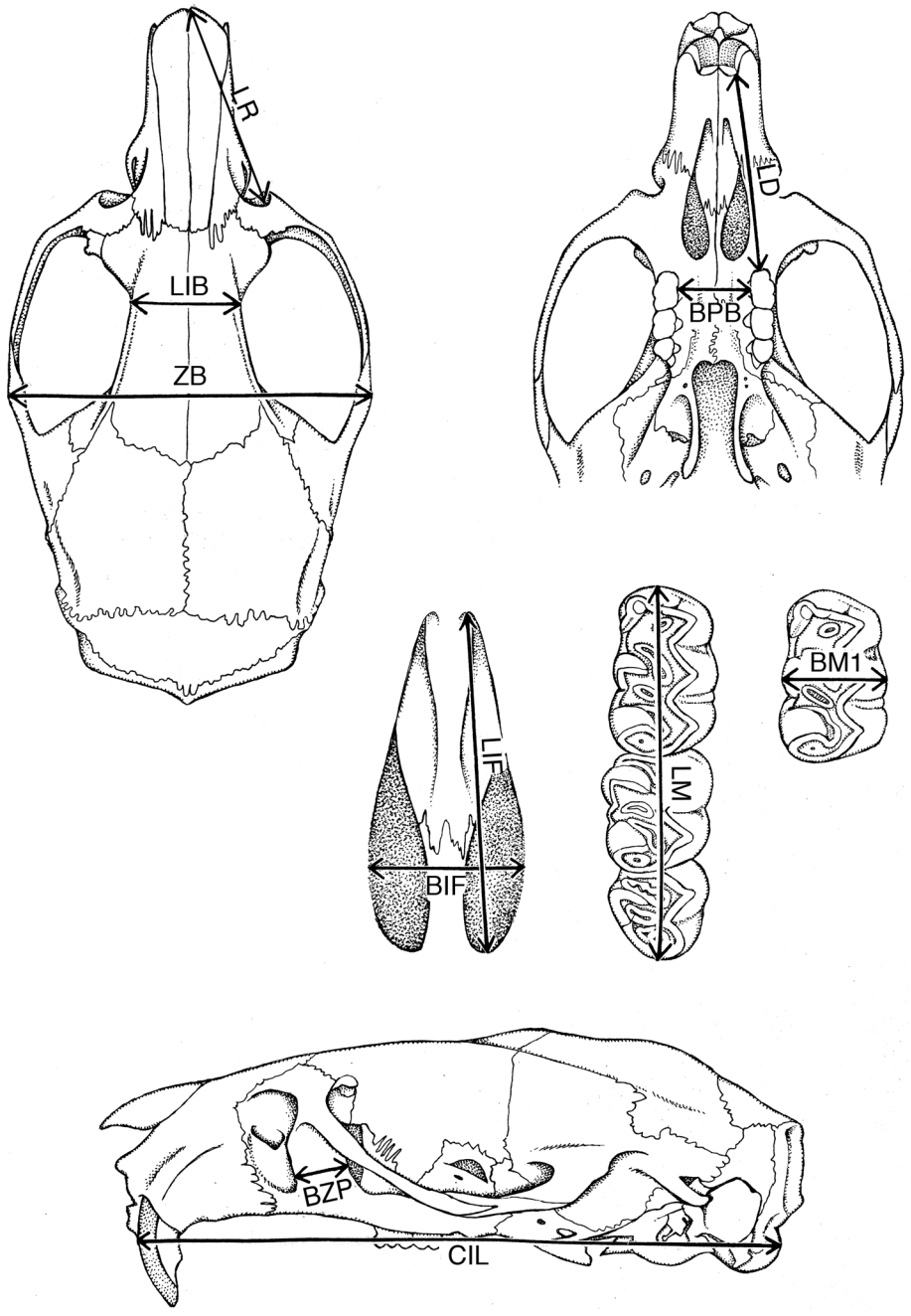

FIG. 1. Limits of craniodental measurements defined in the text.

We report estimates of central tendency and dispersion (for measurements and ratios of measurements) as the sample mean plus or minus one sample standard deviation. We used Welch's *t*-test to evaluate mean differences between species; this univariate two-sample test does not assume equal variances, and it is more robust to differences in sample size and dispersion (provides better control of Type 1 error rates; Delacre et al., 2017) than the more traditionally used Student's *t*-test.

Taxon sampling: Given the phylogenetic objective of this report, we selected one exemplar for each species of *Oecomys* currently recognized as valid, together with an exemplar of the western Amazonian population of *O. paricola* (herein described as a new species) and an exemplar of *O. trabeatus* (herein revalidated). Whenever possible, we selected exemplars collected near type localities, and (all else being equal) we selected exemplars with museum-cataloged voucher specimens. Of the 60 gene sequences in our multigene data matrix (appendix 1), 33 were newly obtained by us, and the remainder were downloaded from GenBank. Unfortunately, many GenBank sequences of *Oecomys* are misidentified, of which those attributed to *O. concolor* and *O. trinitatis* merit brief discussion.

Multiple gene sequences in GenBank are identified as *Oecomys concolor*, but most were obtained from specimens collected far outside the known distribution of this species (Carleton and Musser, 2015: map 207). These misidentifications are based on obsolete nomenclatural usage that has yet to be purged from museum databases and specimen labels. In particular, Hershkovitz's (1960) concept of *O. concolor* included—as subspecies or junior synonyms—at least eight taxa that are currently regarded as valid species, including *O. auyantepui*, *O. catherinae*, *O. flavicans*, *O. mamorae*, *O. roberti*, *O. speciosus*, *O. superans*, and *O. trinitatis*. In consequence, of 40 gene sequences in GenBank currently identified as *O. concolor*, only three cytochrome *b* fragments (each comprising 801 bp) appear to be correctly identified. These three sequences (HM594614, HM594615, HM594617) are from specimens collected in the Rio Negro basin of Amazonas, Brazil; although we have not seen the corresponding voucher specimens (now at INPA), at least one of them (with field number JLP 16806), was identified by the late G.G. Musser, whose research notes are archived in the AMNH Department of Mammalogy. However, all three sequences have a premature stop codon (AGA, at positions 691–693), which suggests that they could represent nuclear pseudogenes. Although these sequences have been included in several recent phylogenetic analyses (e.g., Rocha et al., 2018; Suárez-Villota et al., 2018; Saldanha and Rossi, 2021), the presence of stop codons was not mentioned in any article. Given the problematic homology of these sequences, we did not include them in our analyses.

The name *Oecomys trinitatis* has long been used in the inclusive sense of Musser and Carleton (1993), who included *O. catherinae* among its other alleged synonyms, and this name has also been misapplied to *O. galvez* (see Voss et al., 2024: 78–79). Insofar as can be determined, none of the 11 nucleotide sequences currently deposited as *O. trinitatis* in GenBank—some of which were analyzed, inter alia, by Patton and da Silva (1995), Patton et al. (2000), Weksler (2003), Percequillo et al. (2011), and Steppan and Schenk (2017)—are correctly identified. None can be confidently associated with the morphologically distinctive nominotypical population from Trinidad nor with the morphologically similar forms that occur on the adjacent mainland of northeastern Venezuela.

TABLE 2. Primers used to amplify CYTB, IRBP, and FGB from fresh tissue.

CYTB (ROM):	
LGL 765	5'-GAA AAA CCA YCG TTG TWA TTC AAC T-3'
LGL 766	5'-GTT TAA TTA GAA TYT YAG CTT TGG G-3'
CYTB (Siena College):	
CYTB-MVZ05	5'-CGA AGC TTG ATA TGA AAA ACC ATC GTT G-3'
CYTB-MVZ16	5'-AAA TAG GAA RTA TCA YTC TGG TTT RAT-3'
IRBP (ROM and Siena College):	
IRBP-A1	5'-ATG CGG AAG GTC CTC TTG GAT AAC-3'
IRBP-F	5'-CTC CAC TGC CCT CCC ATG TCT-3'
FGB (ROM):	
BFib17L	5'-TCC CCA GTA GTA TCT GCC ATT AGG GTT-3'
BFib17U	5'-GGA GAA AAC AGG ACA ATG ACA ATT CAC-3'
FGB (Siena College):	
i7FGB-Bfib	5'-CAC AAC GGC ATG TTC TTC AGC AC-3'
i7FGB-B17	5'-ACC CCA GTA GTA TCT GCC GTT TGG AT-3'

DNA extraction and sequencing: New sequence data for this study were obtained at the Royal Ontario Museum (ROM) and Siena College. At both institutions, DNA was extracted from fresh tissue[5] using Qiagen DNeasy Blood & Tissue Kits (QIAGEN) following the manufacturer's instructions and eluted with 100 µL of AE buffer. Historical DNA was extracted at Siena College following the protocol described in Giarla and Voss (2020). Primer sequences used for PCR amplification are listed in tables 2 and 3. At the ROM, each 25 µL PCR reaction consisted of 1 µL of template DNA, 18.89 µL ddH2O, 2.5 µL 10X PCR buffer (Invitrogen), 1.25 µL $MgCl_2$ (Invitrogen), 0.56 µL dNTPs [10 mM], 1 µL [0.01 mM] each of the primers and 0.05 µL Platinum Taq (Invitrogen). At Siena College, each 25 µL PCR reaction consisted of 1 µL of template DNA, 9 µL ddH2O, 1 µL [0.01 mM] each of the primers, and 13 µL GoTaq Green Master Mix (Promega). For amplification of cytochrome *b* (CYTB) from historical samples, the gene was amplified in pieces, with primers designed to amplify overlapping 250–400 bp segments (table 3). For these historical samples, PCR thermocycling conditions consisted of an initial hot start of 94° C for 2 min, followed by 35–40 cycles of denaturation at 94° C for 1 min, annealing at 50°–55° C for 30 s, and extension at 72° C for 30 s, with a final extension at 72° C for 7 min. For amplification of CYTB from fresh tissues, PCR thermocycling conditions consisted of an initial hot start of 94° C for 2 min, followed by 35–40 cycles of denaturation at 94° C for 1 min, annealing at 50°–55° C for 1 min, and extension at 72° C for 1 min, with a final extension at 72° C for 7 min (Lim et al., 2008). For interphotoreceptor retinoid-binding protein (IRBP), PCR thermocycling conditions were an initial hot start of 94° C for 5 min, followed by 40 cycles of denaturation at 94° C for 30 s, annealing at 55°–60° C for 30 sec, and

[5] By "fresh" tissue we mean tissue preserved in the field, either in liquid nitrogen, ethanol, or specially compounded buffer solutions, for the purpose of molecular analysis. "Historical" tissues were harvested from dried skins or skulls of traditionally prepared museum specimens.

TABLE 3. Primers used to amplify CYTB from historical tissues.

OecoCytb-12F	5'-ACG AAA AAC CCA CCC ACT ACT-3'
OecoCytb-391R	5'-AGC CTA CGA ATG CTG TTG CT-3'
OecoCytb-192F	5'-CTC AGT CAC CCA CAT CTG CC-3'
OecoCytb-441R	5'-TGT GAT GAC TGT GGC TCC TC-3'
OecoCytb-200F	5'-CTC ACA TCT GCC GAG ACG TT-3'
OecoCytb-245F	5'-TTC ATG CTA ACG GGG CTT CC-3'
OecoCytb-444R	5'-GTT TGT GAT GAC TGT GGC TCC-3'
OecoCytb-614R	5'-GAG CCG GTT TCG TGT AGG AA-3'
OecoCytb-372F	5'-AGC AAC AGC ATT CGT AGG CT-3'
OecoCytb-800R	5'-TGT GCT GGA GTG TTT AGT GGA-3'

extension at 72° C for 45 s, with a final extension at 72° C for 5 min (Suárez-Villota et al., 2018). For beta fibrinogen (FGB), PCR thermocycling conditions were an initial denaturation of 94° C for 2 min, followed by 40 cycles of denaturation at 94° C for 1 min, annealing at 48°–60° C for 1 min, and extension at 72° C for 1 min, with a final extension at 72° C for 10 min (Ammerman et al., 2012). PCR products were subsequently visualized using 1% agarose gel. Only amplicons with single, intense bands were sequenced. At the ROM, bands were extracted and filtered through a spin column; PCR products were then bidirectionally sequenced and run on an ABI 3730 capillary sequencer (Applied Biosystems, Inc.). Each sequencing reaction consisted of 2 μL of PCR product along with 5 μL ddH_20, 2 μL 5X sequencing buffer (Invitrogen), 0.5 μL primer, and 0.5 μL BIG DYE 3.1 reagent (Applied Biosystems, Inc). The thermocycling profile for sequencing was an initial hot start at 96° C for 1 min, followed by 30 cycles of denaturation at 96° C for 10 s, annealing at 50° C for 5 s, and an extension at 60° C for 4 min. At Siena College, PCR reaction mixtures were enzymatically purified using ExoSAP-IT (ThermoFisher) and sent to GENEWIZ (South Plainfield, NJ) for bidirectional Sanger sequencing.

DNA sequences for all three genes were aligned with MAFFT v7.309 (Katoh and Standley, 2013) and concatenated in Geneious R9 (Biomatters Inc.). We added GenBank sequences from *Hylaeamys megacephalus* (MG323696, MG323617, MG323788) for rooting purposes, resulting in a data matrix with 25 species. We conducted both maximum-likelihood (ML) and Bayesian phylogenetic analyses with datasets partitioned by gene. We used IQ-TREE v2.3.6 (Minh et al., 2020) to simultaneously test gene-partitioning schemes, fit nucleotide substitution models, and infer the ML tree. Nodal support was estimated with 1000 ultrafast bootstrap replicates (ufBOOT; Minh et al., 2013). We inferred a Bayesian tree by applying the best-fitting nucleotide substitution models and partitioning scheme from the IQ-TREE analysis using MrBayes v3.2.7a (Ronquist et al., 2012). We unlinked model parameters between the partitions and conducted two independent runs, each consisting of 20 million generations and 4 MCMC chains. After checking for stationarity in Tracer v1.7.1 (Rambaut et al., 2018), the posterior distribution of trees was summarized using the "sumt" command in MrBayes to create a consensus tree.

GenBank accession numbers for all the sequence data analyzed in this report are listed in appendices 1–3.

Karyotypic analysis: We report previously unpublished karyotypic information for several specimens collected many years ago in Venezuela. Mitotic metaphase cell suspensions, prepared in the field using minor modifications of Patton's (1967) colchicine/hypo-

tonic citrate method, were frozen in liquid nitrogen for transport to the AMNH, where they were processed for standard karyotypic analysis. Fundamental numbers (counts of autosomal arms) could not be determined from female karyotypes because the sex chromosomes were not identifiable.

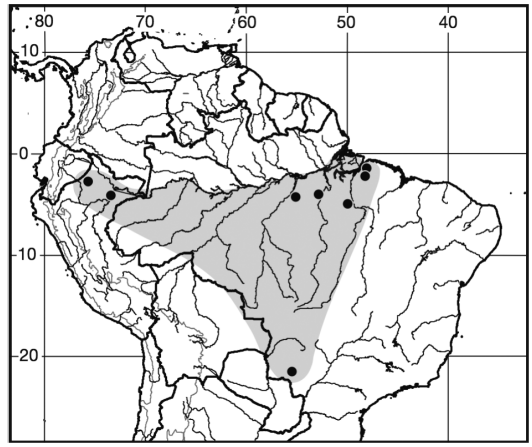

FIG. 2. Geographic range of *Oecomys paricola* as illustrated by Carleton and Musser (2015).

A NEW SPECIES FROM WESTERN AMAZONIA

The geographic range of *Oecomys paricola*, as that species is currently recognized (Carleton and Musser, 2015), extends from eastern Amazonia to western Amazonia and southward almost to Paraguay (fig. 2). This immense territory spans the main biogeographic axes of Amazonia—the Amazon River, the Rio Negro, and the Rio Madeira (Wallace, 1854)—and it crosses the ecologically important boundary between Amazonia and the Cerrado. Few species of small nonvolant mammals are so widely distributed in tropical South America, and none with such extensive distributions fail to exhibit deep phylogeographic structure when interrogated with genetic data.

In fact, the museum specimens currently referred to *Oecomys paricola* represent three widely disjunct geographic series. The first consists of multiple localities scattered along the south bank of the lower Amazon from the Tapajós to the Atlantic coast of Brazil; the second consists of several localities in northeastern Peru and eastern Ecuador; and the third is Maracajú, a locality in the Brazilian state of Mato Grosso do Sul. The latter is easily eliminated from further consideration. We examined the specimens from Maracajú (AMNH 134510, 134511) that Carleton and Musser (2015) identified as *O. paricola* and determined that they are misidentified examples of *O. cleberi*: both specimens exhibit the diagnostic traits of the latter species as discussed by Rocha et al. (2012) and Brandão et al. (2024).[6] There remains only the question as to whether the specimens from northeastern Peru and eastern Ecuador are conspecific with specimens from eastern Brazil. For the reasons summarized below, we conclude that they are not.

[6] Noteworthy morphological differences between *Oecomys cleberi* and *O. paricola* include: (1) ventral pelage color (mostly self-white in *O. cleberi* versus mostly gray-based in *O. paricola*), (2) relative tail length (LT/HBL, about 1.06 on average in *O. cleberi* versus 1.20 in *O. paricola*), (3) ungual tufts on digits II–V of the hind foot (denser and longer in *O. cleberi* than in *O. paricola*), (4) incisive foramina (extending posteriorly to or between the M1 crowns in *O. cleberi*, but not in *O. paricola*), and (5) palatal length (visibly shorter in *O. cleberi* than in *O. paricola*).

Oecomys hiceae, new species

Oecomys paricola: Hice and Velazco, 2012: 57 (a misidentification, not *paricola* Thomas, 1904).
Oecomys rutilus: Gomes et al. 2016: 416, 426 (a misidentification associated with cytochrome oxidase subunit I [COI] sequence data deposited in GenBank with accession number EU095453 [voucher = ROM 104473], not *rutilus* Anthony, 1921).

Type material and type locality: The holotype (TTU 101036) consists of the skin, skull, and frozen tissues of an adult female collected by Christine L. Hice (original number CLH 2069) on 28 December 1997 at the Estación Biológica Allpahuayo, 28 km southwest of Iquitos on the road from Iquitos to Nauta in Loreto department, Peru. According to Hice and Velazco (2012), the biological station is in the Reserva Nacional Allpahuayo-Mishana with coordinates 3°58′S, 73°25′W.

Distribution: *Oecomys hiceae* is known from specimens collected north of the Amazon River in Loreto department, Peru, and in Orellana province, Ecuador (fig. 3).

Description: The dorsal pelage of *Oecomys hiceae* is 8–9 mm long and finely grizzled tawny or reddish brown in fully adult specimens (the coloration is duller in juveniles and subadults). The ventral pelage is abruptly paler, gray-based whitish over the abdomen in some specimens (e.g., KU 158190) and gray-based buffy in others (e.g., TTU 101036), but one specimen (MUSM 44980, a subadult) has uniformly self-white ventral fur and another (TTU 98907, an older adult) has self-buffy abdominal fur. Even specimens with gray-based abdominal fur, however, have self-white fur on the chin, throat, chest, and groin. The ears are covered with short brownish hairs that do not contrast sharply with the color of the head in fully adult specimens (but TTU 101252, a juvenile, has darker, almost blackish ears). The tail (117% of head-and-body length, on average) is uniformly dark except for an indistinctly paler ventral region near its base; the caudal scales (about 19 rows/cm on most specimens) are clearly visible all the way to the tip, which has a terminal tuft of longer hairs measuring 6–8 mm. The hind feet are pale (buffy or pale orange) over the ankles and proximal metatarsals, but the distal metatarsals are distinctly darker; the ungual tufts do not exceed the claws in length on any examined specimen. No fluid-preserved male specimens are currently available for dissection, so the preputial gland morphology (taxonomically informative in *Oecomys*; Voss et al., 2024) is unknown.

In dorsal cranial view (fig. 4) the rostrum is flanked at its base by shallow zygomatic notches, and the interorbital region is anteriorly convergent with well-developed supraorbital crests; small postorbital processes can be seen on the holotype, but they are less distinct on other specimens. The supraorbital crests are continuous with temporal crests that are distinct along the parietal-squamosal sutures on each side of the skull, but these crests are sometimes indistinct where they cross the parietals behind the squamosal zygomatic processes; at this point on either side, the parietal broadly extends onto the lateral braincase, more or less filling the space between the temporal crest and the postzygomatic ridge. In ventral cranial view, the incisive foramina are wide (BIF/LIF = 0.47 ± 0.03) and moderately long (LIF/LD = 0.61 ± 0.01), but they do not extend posteriorly to or between the molar rows. Sphenopalatine vacuities are consistently absent. An alisphenoid strut (separating the buccinator-masticatory and accessory oval foramina; fig. 5A) is bilaterally present in seven of the

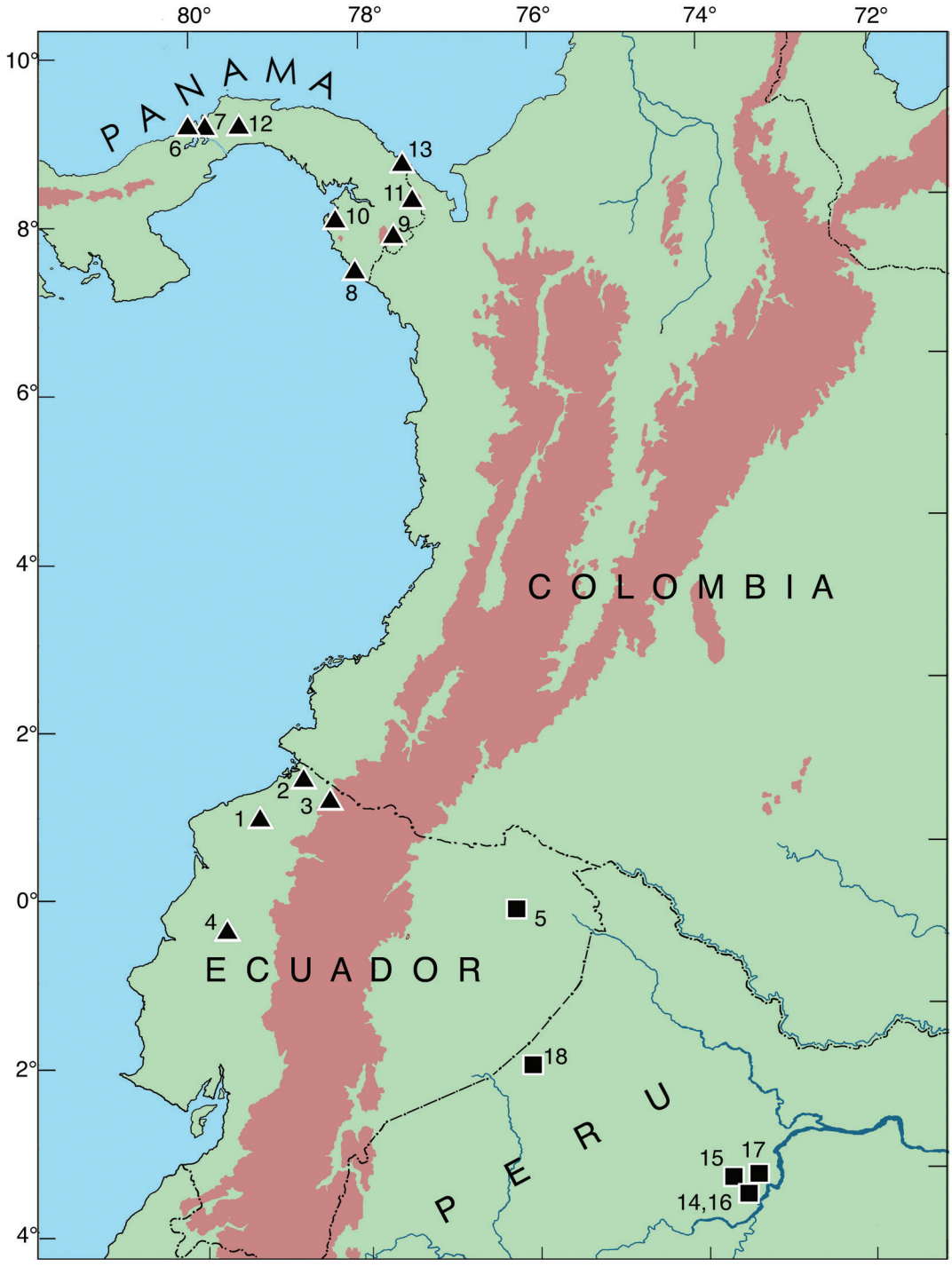

FIG. 3. Geographic distribution of *Oecomys hiceae* (squares) and *O. trabeatus* (triangles) as documented by specimens examined for this report. Elevations >1000 m are shaded.

FIG. 4. Dorsal, ventral, and lateral views of crania of *Oecomys hiceae* (TTU 101036, holotype) and *O. paricola* (USNM 461390). All views about ×2.0.

eight adult specimens we scored for this trait; the unique exception (TTU 98807) has an alisphenoid strut on just one side. The stapedial arterial circulation is complete, with a well-developed supraorbital branch (pattern 1 of Voss, 1988). Above the auditory bulla, the postglenoid foramen is large and widely open; the tegmen tympani narrowly contacts the posterior margin of the squamosal in some specimens but not in others. The hamular process of the squamosal is usually short and broad, constricting the subsquamosal fenestra to an inconspicuous notch in most specimens, but not fully occluding it. The mastoid capsules are fenestrated in some specimens (e.g., TTU 98907), but not in others (e.g., TTU 101036). The molar dentition appears to lack any distinctive occlusal features, but an accessory labial root is consistently present above the paracone of M1.

Karyotype: No chromosomal information is available for this species.

Comparisons: *Oecomys hiceae* and *O. paricola* are morphometrically indistinguishable, with overlapping measurements for all external and craniodental dimensions, although mean differences in ear length (Ear) and crown length of the upper molar row (LM) are statistically significant (table 4). Similarly, we have not found any external feature by which these taxa can be reliably distinguished. Cranial comparisons, however, provide several points of difference.

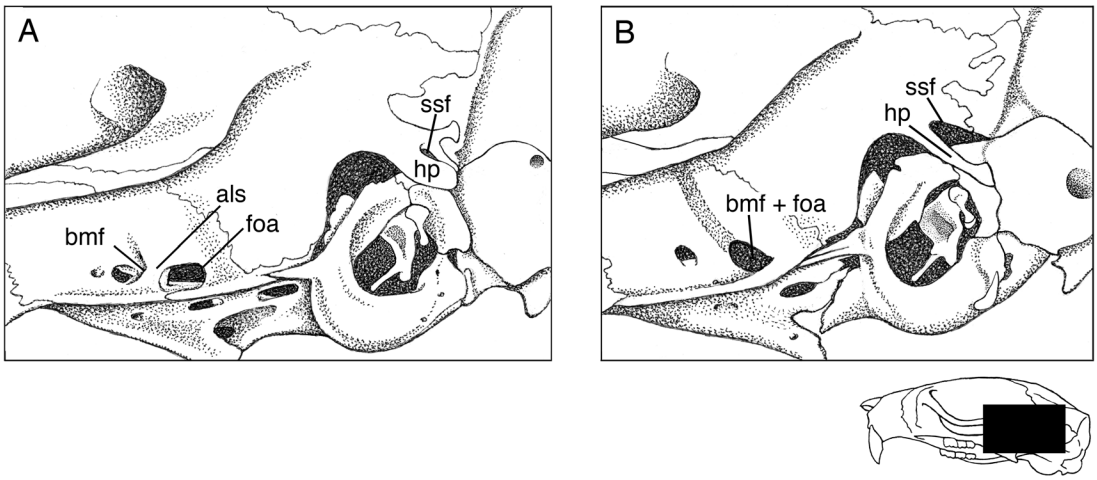

FIG. 5. Ventrolateral cranial views of *Oecomys hiceae* (**A**, TTU 101036) and *O. paricola* (**B**, USNM 461389). A bony strut of the alisphenoid (**als**) separates the buccinator-masticatory foramen (**bmf**) from the foramen ovale accessorius (**foa**) in most specimens of *O. hiceae*, whereas the alisphenoid strut is consistently absent and the buccinator-masticatory and accessory oval foramina are confluent in *O. paricola*. Additionally, the hamular process of the squamosal (**hp**) is typically short and broad in *O. hiceae*, reducing the subsquamosal fenestra (**ssf**) to a small opening; by contrast, the hamular process is usually long and slender, and the subsquamosal fenestra is usually larger in *O. paricola*.

The vertical strut of the alisphenoid that separates the buccinator-masticatory foramen from the accessory oval foramen in many other cricetids is consistently absent in all examined specimens of *Oecomys paricola* that we scored for this trait ($N = 31$), with the result that these foramina are always confluent in lateral cranial view (fig. 5B). By contrast, the alisphenoid strut is present (bilaterally in most specimens, but unilaterally in TTU 98807; see above), such that the buccinator-masticatory and accessory oval foramina are separate openings in *O. hiceae* (fig. 5A). A second, but by no means constant distinction between these species concerns the hamular process of the squamosal, which is typically shorter and broader in *Oecomys hiceae* and sometimes pinches the subsquamosal fenestra to a narrow aperture (fig. 5A), whereas the hamular process in *O. paricola* is often longer and narrower, and the subsquamosal fenestra is correspondingly larger (fig. 5B). A third cranial feature that might distinguish these species are the small postorbital processes that can be seen in dorsal view of the holotype skull of *O. hiceae* (fig. 4). Although indistinct on most other specimens of *O. hiceae*, these small projections are unambiguously absent in all examined material of *O. paricola*. Larger series of *O. hiceae* are needed to properly assess the potentially diagnostic value of this trait.

Despite these minor morphological differences, *Oecomys hiceae* and *O. paricola* are impressively (10%–11%) divergent at the cytochrome *b* locus (table 5), and phylogenetic analyses of our multigene dataset suggest that these species are not closely related (see below).

Habitat: All known collection localities for *Oecomys hiceae* are in the rainforested Amazonian lowlands. Rainforest vegetation at the Estación Biológica Allpahuayo-Mishana (appendix 4: locality 15) was briefly described by Hice and Velazco (2012), who reported

TABLE 4. External and craniodental measurements (mm) and weights (g) of *Oecomys hiceae* and *O. paricola*.

	O. hiceae[a]	*O. paricola*[b]	Difference[c]
HBL	113 ± 8 (101–119) 4	111 ± 3 (105–115) 14	n.s.
LT	131 ± 8 (120–138) 4	133 ± 8 (120–145) 14	n.s.
HF	24 ± 1 (22–25) 4	24 ± 1 (22–27) 14	n.s.
Ear	15 ± 1 (14–16) 4	17 ± 1 (15–19) 15	*
CIL	25.8 ± 0.7 (25.1–27.2) 6	26.0 ± 0.7 (24.6–27.0) 20	n.s.
LD	7.7 ± 0.3 (7.4–8.1) 6	7.5 ± 0.3 (6.9–8.0) 20	n.s.
LM	4.0 ± 0.1 (3.8–4.2) 9	4.2 ± 0.1 (4.0–4.4) 29	**
BM1	1.2 ± 0.0 (1.1–1.2) 9	1.2 ± 0.0 (1.1–1.2) 28	n.s.
LIF	4.7 ± 0.3 (4.4–5.1) 6	4.8 ± 0.2 (4.5–5.3) 20	n.s.
BIF	2.2 ± 0.1 (2.0–2.4) 6	2.3 ± 0.1 (2.0–2.6) 20	n.s.
BPB	2.9 ± 0.1 (2.8–3.0) 6	2.9 ± 0.2 (2.6–3.2) 20	n.s.
BZP	2.4 ± 0.1 (2.3–2.7) 6	2.5 ± 0.2 (2.2–3.0) 20	n.s.
LIB	5.1 ± 0.2 (4.8–5.6) 7	5.2 ± 0.2 (4.9–5.8) 20	n.s.
ZB	14.8 ± 0.6 (13.8–15.3) 6	15.1 ± 0.5 (14.1–15.9) 19	n.s.
LR	8.6 ± 0.3 (8.3–9.0) 6	8.3 ± 0.3 (7.8–8.9) 20	n.s.
Weight	39 ± 6 (30–45) 5	42 ± 8 (28–60) 15	n.s.

[a] The mean plus or minus one standard deviation, the observed range (in parentheses), and the sample size for measurements of the following series: KU 158190; MUSM 33966, 33967, 44980; ROM 104473; TTU 98907, 101036, 101252, 124958.

[b] The mean plus or minus one standard deviation, the observed range (in parentheses), and the sample size for measurements of the following series: AMNH 188963, 203391, 203392, 203397; BMNH 4.7.4.63 (type), 4.7.4.64, 4.7.4.108; FMNH 136894, 136943, 143288–143292; USNM 393819, 393842, 461385, 461386, 461388–461395, 461400, 545232, 545233.

[c] Results of two-tailed Welch's *t*-tests: n.s. = not significant ($p > 0.05$), * = $p < 0.05$; ** = $p < 0.01$.

that their two specimens (TTU 98907, 101252) were trapped at ground level in *franco arcilloso* (fig. 6) a local habitat that they characterized as transitional between *monte alto* (tall primary forest growing on clay soils) and *varillal* (white sand forest). Subsequent botanical studies (Vásquez and Phillips, 2000; Vormisto et al., 2000) have documented floristic and structural differences among forests growing on different soil types at Allpahuayo-Mishana, but with only two captures of *O. hiceae* it is hard to know whether or not this species is a local habitat specialist.

Parque Nacional Yasuní (appendix 4: locality 5) is the only other locality for which substantial ecological information is available. This globally important protected area (Bass et al., 2010) has been the site of numerous ecological and botanical research projects (e.g., Valencia et al., 2004), but none has focused on the nonvolant small mammals, the local habitats of which remain undocumented. According to Pitman (2000) the natural vegetation of Yasuní includes terra firme forest, seasonally flooded forest (both *várzea* and *igapó*; Prance, 1979), and swamp forest (on permanently waterlogged soils). The two specimens from this locality were both taken in terra firme forest, where one of them (ROM 104473) was trapped on a branch 1.5 m above the ground near a small stream.

TABLE 5. Uncorrected pairwise distances (scaled as percentages) within and among cytochrome *b* sequences of *Oecomys hiceae* and three haplogroups of *O. paricola*[a]

	N	*hiceae*	*paricola* E	*paricola* N	*paricola* W
hiceae	10	1.20 ± 1.12			
paricola E	19	10.17 ± 1.02	0.54 ± 0.27		
paricola N	7	11.05 ± 1.09	3.69 ± 0.59	0.63 ± 0.25	
paricola W	9	10.56 ± 0.98	5.07 ± 0.68	5.12 ± 0.69	1.38 ± 1.22

[a] Table entries are means plus or minus one standard deviation. Haplogroup abbreviations (after Suárez-Villota et al. (2018): E = "eastern clade," N = "northern clade," W = "western clade."

Remarks: We analyzed sequence data from ROM 106213, (appendix 2), but the voucher material has been lost. The only phenotypic data for this specimen, a fluid-preserved male, are external measurements (HBL, 89 mm; LT, 115 mm; HF, 22 mm; Ear, 14 mm; weight, 28 g). These values are either substantially smaller than those we recorded from our sample of adult individuals (HBL, LT, weight), or they just match those of the smallest adults we measured (HF, Ear; table 4). From these comparisons we infer that ROM 106213 was immature, but there can be no doubt of its taxonomic identification given the trivial genetic distance (<1%, uncorrected) between the cytochrome *b* sequences we obtained from tissues of this specimen and from ROM 104473 (taken at the same locality).

Etymology: For Christine L. Hice, whose collections of small mammals—marsupials, bats, and rodents—from Loreto, Peru, are among the largest ever made in western Amazonia. Preserved at the LACM, MUSM, and TTU, and only partially monographed to date (Hice et al., 2004; Hice and Velazco, 2012), Chris's specimens are an indispensable resource for Amazonian biodiversity research and will be consulted by taxonomists for many years to come.

Specimens examined (*N* = 9): **Ecuador**—*Orellana*, Parque Nacional Yasuní (ROM 104473). **Peru**—*Loreto*, El Triunfo (MUSM 33966, 33967), Estación Biológica Allpahuayo (TTU 98907, 101036, 101252), La Habana (TTU 124958), Llanchama (MUSM 44980), San Jacinto (KU 158190).

Other specimens examined (*Oecomys paricola*, *N* = 33): **Brazil**—*Pará*, Agrovila da União (USNM 521529), 52 km S Altamira (USNM 549531, 549532), Belém (USNM 393819, 393842, 461386, 545232, 545233), BR 10 Km 87–94 (FMNH 136943, 136894, 143288–143292), BR 165 Km 217 (USNM 544601), Capím (AMNH 188963, 203391, 203392, 203397; USNM 461385, 461388–461395, 461400), Igarapé Açu (BMNH 4.7.4.63 [holotype]), Porto Jatobal (USNM 519734, 521453, 521528).

A REVALIDATED SPECIES FROM PANAMA AND WESTERN ECUADOR

Another species with an improbably wide geographic distribution is *Oecomys bicolor*. As recognized by Carleton and Musser (2015: map 204), this species occurs throughout Amazonia, in the coastal sierras of northern Venezuela, and west of the Andes in Ecuador and Panama. The type locality of *Oecomys bicolor* is in eastern Ecuador, from which genetic data were long unavailable. Recently, however, Voss et al. (2024) analyzed cytochrome *b* sequences from eastern Ecua-

FIG. 6. Habitat of *Oecomys hiceae* at the Estación Biológica Allpahuayo-Mishana, Loreto, Peru. This habitat, locally known as *franco arcilloso*, is said to be intermediate in character between tall primary forest growing on clay soil (*monte alto*) and white sand forest (*varillal*); all three forest types are found at this locality. Photo by Christine L. Hice (date unkown).

dor and numerous other localities in western Amazonia. Phylogenetic analyses revealed that these sequences formed two distinct haplogroups, one of which (the nominotypical "northern clade") is present in eastern Ecuador and northeastern Peru, and another (the "southern clade") is found in southeastern Peru. Both clades also occur in western Brazil, where Patton et al. (2000) had previously reported them from separate localities along the Rio Juruá). Although these haplogroups are substantially divergent, they seem to be phenotypically and karyotypically indistinguishable (Patton et al., 2000; Voss et al., 2024). By contrast, trans-Andean specimens—those collected in Panama and western Ecuador—differ from Amazonian specimens in morphology and mitochondrial DNA as summarized in the account that follows.

Oecomys trabeatus G.M. Allen and Barbour, 1923

Rhipidomys dryas Thomas, 1900: 271. Type locality: "Paramba" (= Hacienda Paramba), Imbabura province, Ecuador. This is an unavailable name preoccupied by *Oryzomys dryas* Thomas, 1898.
Oryzomys (*Oecomys*) *dryas*: Thomas, 1906: 445 (name combination).

Oecomys trabeatus G.M. Allen and Barbour, 1923: 262. Type locality: "Rio Jesusito," Darién province, Panama.

Oecomys endersi Goldman, 1933: 525. Type locality: "Barro Colorado Island," Panamá province, Panama.

Oryzomys (*Oecomys*) *bicolor trabeatus*: Hershkovitz, 1960: 533 (name combination).

Oryzomys (*Oecomys*) *bicolor occidentalis* Hershkovitz, 1960: 533 (replacement name for *Rhipidomys dryas* Thomas, 1900; see above).

Oryzomys (*Oecomys*) *bicolor bicolor*: Cabrera, 1961: 403, part (*dryas* included as a synonym; not *Hesperomys bicolor* Tomes, 1860).

Oecomys bicolor: Musser and Carleton, 1993: 715, part (*dryas*, *endersi*, *occidentalis*, and *trabeatus* included as synonyms; not *Hesperomys bicolor* Tomes, 1860).

Distribution: Examined specimens of *Oecomys trabeatus* document a geographic range that extends from central Panama to western Ecuador (fig. 3). Recorded elevations are from sea level to almost 800 m. Although we have not seen any material from western Colombia, we assume that it also occurs there.

Description: The dorsal pelage of *Oecomys trabeatus* is 8–11 mm long, finely grizzled, and tawny to reddish-brown in fully adult specimens. The ventral pelage is abruptly self-white—the hairs white to their roots—from chin to anus, including the insides of the forelimbs and hind limbs; a thin line of clear ochraceous fur separates the dorsal and ventral color zones along the flanks of some specimens. The ears are covered with short brownish hairs and do not contrast in color with the fur of the head. The hind feet are mostly pale (probably whitish or buffy in life), but some specimens have an indistinct patch of darker hairs over the distal metacarpals; the ungual tufts do not exceed the intact pedal claws in length on any examined specimen. The tail is unicolored (all dark), about 119% of head-and-body length (on average), and it has a terminal pencil of longer hairs that usually extend 5–7 mm beyond the fleshy tip; we counted 17–20 scale rows/cm on two fluid specimens.[7] The same two specimens (MSB 222113, 222115), both males, have large preputial glands that extend beyond the ventral flexure of the penis to lie between the skin and the abdominal musculature.

In dorsal cranial view (fig. 7), the short rostrum (LR/CIL = 0.33 ± 0.01) is flanked by shallow zygomatic notches. The supraorbital crests are smoothly continuous with low temporal crests that extend along the dorsolateral braincase following the parietal-squamosal sutures to a point on each side just behind the squamosal zygomatic root; beyond this point, the parietal broadly extends onto the lateral braincase, more or less filling the space between the temporal crest and the postzygomatic ridge. In ventral cranial view, the incisive foramina are variably wide (BIF/LIF = 0.48 ± 0.05) and moderately long (LIF/LD = 0.62 ± 0.02), but they do not extend posteriorly to or between the first upper molars. Although the roof of the mesopterygoid foramen is almost entirely ossified, small sphenopalatine vacuities are occasionally present. Alisphenoid struts (separating the buccinator-masticatory and accessory oval foramina) are bilaterally present in 15 of the 16 specimens that we scored for this trait; the unique exception (ANSP 19687) lacks an alisphenoid strut on both sides of the skull. The stapedial circulation is complete, with a well-

[7] Although Allen and Barbour (1923: 263) described the tail of the holotype (MCZ 19837) as "slightly tufted," no terminal pencil of distinctly longer (>3 mm) hairs is now visible on that specimen.

FIG. 7. Dorsal, ventral, and lateral views of crania of *Oecomys trabeatus* (MSB 222115) and *O. bicolor* (AMNH 272727). All views ca. ×2.0.

developed supraorbital branch (pattern 1 of Voss, 1988). Above the auditory bulla, the postglenoid foramen is large and widely open. The tegmen tympani either does not contact the posterior margin of the squamosal (in 7 of 12 specimens scored bilaterally for this trait) or makes narrow contact on one or both sides; no examined specimen exhibits broad petrosal-squamosal overlap. Behind the hamular process of the squamosal, the subsquamosal fenestra is usually small but distinct. Each mastoid capsule is usually perforated by a small fenestra. The dentition appears to lack any distinctive occlusal features, but M1 lacks an accessory labial root.

Karyotype: No chromosomal information is available for this species.

Comparisons: *Oecomys trabeatus* differs from *O. bicolor* in several aspects of external morphology. The dorsal fur is much longer (9 ± 1 mm, $N = 11$) in *O. trabeatus* than it is in *O. bicolor* (5 ± 1 mm, $N = 35$), and this difference is visually and tactilely obvious in side-by-side comparisons of exemplar skins. Additionally, *O. trabeatus* has significantly larger ears than *O. bicolor* (table 6), and the tail of *O. trabeatus* is relatively longer (LT/HBL = 1.19 ± 0.11, $N = 12$) than that of *O. bicolor* (LT/HBL = 1.07 ± 0.09, $N = 31$); both differences are visually obvious in most exem-

TABLE 6. External and craniodental measurements (mm) and weights (g) of *Oecomys trabeatus* and *O. bicolor*.

	O. trabeatus[a]	*O. bicolor*[b]	Difference[c]
HBL	108 ± 8 (95–118) 12	102 ± 8 (82–117) 31	n.s.
LT	128 ± 8 (116–142) 12	109 ± 8 (90–122) 31	***
HF	23 ± 1 (21–24) 18	22 ± 1 (19–24) 36	**
Ear	15 ± 1 (12–17) 14	13 ± 1 (11–15) 30	***
CIL	24.9 ± 0.8 (23.4–26.0) 15	24.4 ± 0.9 (22.1–25.8) 34	n.s.
LD	7.2 ± 0.4 (6.2–8.0) 17	7.0 ± 0.4 (5.9–7.6) 36	n.s.
LM	3.9 ± 0.1 (3.8–4.1) 19	3.8 ± 0.1 (3.7–4.0) 41	n.s.
BM1	1.1 ± 0.0 (1.1–1.2) 19	1.1 ± 0.0 (1.1–1.2) 41	n.s.
LIF	4.4 ± 0.3 (3.7–5.0) 17	4.6 ± 0.2 (4.1–5.0) 36	n.s.
BIF	2.1 ± 0.3 (1.8–2.8) 16	2.1 ± 0.1 (1.8–2.3) 37	n.s.
BPB	2.7 ± 0.1 (2.4–3.0) 15	2.7 ± 0.2 (2.4–3.1) 36	n.s.
BZP	2.3 ± 0.2 (1.9–2.6) 17	2.2 ± 0.1 (1.9–2.5) 37	*
LIB	4.8 ± 0.3 (4.4–5.3) 17	4.8 ± 0.2 (4.5–5.2) 37	n.s.
ZB	14.6 ± 0.7 (13.3–15.4) 13	14.2 ± 0.5 (13.1–15.4) 36	n.s.
LR	8.2 ± 0.5 (7.4–9.0) 16	7.8 ± 0.3 (7.0–8.4) 34	**
Weight	37 ± 2 (35–40) 5	31 ± 6 (19–42) 32	***

[a] The mean plus or minus one standard deviation, the observed range (in parentheses), and the sample size for measurements of the following series: ANSP 19687–19689, 19691, 19692; BMNH 99.12.5.3, 99.12.5.4 (type of *dryas*), 1.3.19.7, 15.1.1.56; MCZ 19837 (type of *trabeatus*); MSB 222113, 222115; USNM 113289, 113290, 306949, 306950, 335530, 335531, 335534.

[b] From western Amazonia (the "northern clade" identified by Voss et al., 2024). The mean plus or minus one standard deviation, the observed range (in parentheses), and the sample size for measurements of the following series: AMNH 67404, 67405, 268257, 268258, 272674, 272710, 272724, 272727, 273064, 273096; BMNH 7.1.1.96 (holotype); MUSM 13315, 13316, 13318, 13319, 15333, 15334; ROM 104505, 105519, 105597, 105560, 118873, 118884, 118911, 106153;TTU 84901, 85228, 98621, 98766, 98829, 100834, 124942, 124943, 124945, 124947, 124949–124952, 124954, 124960.

[c] Results of two-tailed Welch's *t*-tests: n.s. = not significant ($p > 0.05$), * = $p < 0.05$; ** = $p < 0.01$, *** = $p < 0.001$.

plar comparisons. Most specimens of *O. trabeatus* also have a distinct terminal pencil of long hairs that project about 5–7 mm beyond the fleshy tip, whereas most specimens of *O. bicolor* lack a distinct terminal pencil. Although statistical tests suggest that *O. trabeatus* has significantly longer hind feet than *O. bicolor*, this difference (if not artifactual) is not visually apparent.

Craniodental comparisons of *Oecomys trabeatus* and *O. bicolor* are less productive, because these species are similar in craniodental measurements and appearance (table 6, fig. 7). Nevertheless, *O. trabeatus* has incisive foramina that are—on average—shorter in relation to diastema length (LIF/LD = 0.62 ± 0.02, N = 15) and that never extend posteriorly to or between the first upper molars (M1), whereas *O. bicolor* has incisive foramina that are relatively longer (LIF/LD = 0.66 ± 0.02, N = 36) and often extend posteriorly to or between the first molars. Additionally, alisphenoid struts (separating the buccinator-masticatory and accessory oval foramina on each side) are almost always bilaterally present in *O. trabeatus*, whereas alisphenoid struts are frequently absent on one or both sides in specimens of *O. bicolor* (table 7). Although statistical tests suggest that there are significant differences between *O. trabeatus* and *O. bicolor* in breadth of the zygomatic plate and rostral length

TABLE 7. Observed frequencies of the alisphenoid strut in adult specimens of *Oecomys trabeatus* and *O. bicolor*.

	O. trabeatus	*O. bicolor*[a]
Present on both sides	15 (94%)	11 (29%)
Present on one side	—	7 (18%)
Absent on both sides	1 (6%)	20 (53%)
Totals:	16	38

[a] The nominotypical northern clade (Voss et al., 2024).

(table 6), taxonomic differences in these dimensions are not visually apparent in side-by-side comparisons. The only other noteworthy phenotypic difference between these species concerns the preputial glands, which are large in *O. trabeatus* but are not macroscopically visible in specimens belonging to the nominotypical mtDNA clade of *O. bicolor* (see Voss et al., 2024: 64).

Genetic comparisons of *Oecomys trabeatus* and *O. bicolor* are limited by available data (the karyotype of *O. trabeatus* is unknown), but uncorrected pairwise sequence differences at the cytochrome *b* locus (table 8) reveal that *Oecomys trabeatus* is highly divergent (ca. 8%–9%) from both of the western Amazonian haplogroups of *O. bicolor*, and the phylogenetic analyses reported below suggest that these species are not closely related.

Habitats: The holotype was captured in lowland rainforest along the Río Jesusito in eastern Panama (fig. 8), and all other known collection localities for this species are also in rainforested (or formerly rainforested) landscapes; recorded elevations range from near sea level (e.g., at Guayabo, on the Pacific coast of Darién province, Panama; appendix 4: locality 8) to almost 800 m (at Hacienda Paramba in the western Andean foothills of Imbabura province, Ecuador; appendix 4, locality 3). Detailed ecological and floristic descriptions, together with photographs of local habitats, are available for Barro Colorado Island, Panama (Croat, 1978; Leigh et al., 1996) and the Centro Científico Río Palenque, Ecuador (Dodson and Gentry, 1978).[8]

Remarks: Although we have not seen the holotype of *Oecomys endersi* (at UMMZ), we examined nearly topotypical material (MSB 222113, 222115), and Goldman's (1933) description and measurements fall within the range of variation exhibited by the material listed below.

Specimens examined ($N = 26$): **Ecuador**—*Esmeraldas*, Pambilar (USNM 113289, 113290), San Javier (BMNH 1.3.19.7); *Imbabura*, Paramba (BMNH 99.12.5.3, 99.12.5.4 [type of *dryas*]); *Los Rios*, 58 km SW Santo Domingo de los Colorados (BMNH 99.12.5.3). **Panama**—*Colón*, Camp Piña (USNM 306381), Parque Nacional Soberanía (MSB 222113, 222115); *Darién*, Guayabo (ANSP 19688–19692), Pelisa (ANSP 19687), Río Jesusito (MCZ 19837 [type]), Tacarcuna Village (USNM 339059); *Panamá*, Cerro Azul (USNM 305706, 306949, 306950); *San Blas*, Quebrada Venado (USNM 335530–335535).

Other specimens examined (*Oecomys bicolor*, $N = 44$): **Ecuador**—*Morona-Santiago* Gualaquiza (BMNH 7.1.1.96 [type]); *Orellana*, 35 km S Pompeya Sur (ROM 105519, 105597, 105660), 38 km S Pompeya Sur (ROM 105329, 118794, 118873), 42 km S and 1 km E Pompeya Sur (ROM 104505, 118884, 118911), Tiputini Biodiversity Station (ROM 106153); *Pastaza*, Canelos (AMNH 67404, 67504), 5 km N Puyo (TTU 84901, 85228). **Peru**—*Amazonas*, vicinity of Huampami on

[8] Barro Colorado Island is the type locality of *Oecomys endersi* (a junior synonym; see above), and it is only a few kilometers from Parque Nacional Soberanía (appendix 4: locality 7). The Río Palenque Science center is on the road from Santo Domingo de los Colorados to Quevedo (appendix 4: locality 4).

Río Cenepa (MVZ 154988, 154990–154992, 154997, 154999, 155001); *Loreto*, Collpa Salvador (MUSM 17571), Estación Biológica Allpahuayo (TTU 98621, 98766, 98829, 100834), Iquitos (TTU 124943), Km 48 on Iquitos-Nauta Highway (TTU 124945), Km 48.3 on Iquitos-Nauta Highway (TTU124951, 124952, 124954), Km 50 on Iquitos-Nauta Highway (TTU 124950), Km 52 on Iquitos-Nauta Highway (TTU 124947, 124949), Km 60.4 on Iquitos-Nauta Highway (TTU 124942), Nina Rumi (MUSM 45737–45743), Pachacutec (MUSM 43188).

TABLE 8. Uncorrected pairwise distances (scaled as percentages) within and among cytochrome *b* sequences of *Oecomys trabeatus* and two haplogroups of *O. bicolor*[a]

	N	*trabeatus*	*bicolor* N	*bicolor* S
trabeatus	2	0.26 ± 0.00		
bicolor N	36	9.13 ± 1.01	1.33 ± 0.74	
bicolor S	18	8.57 ± 1.01	5.67 ± 0.70	1.13 ± 0.60

[a] Table entries are means plus or minus one standard deviation. Haplogroup abbreviations (after Voss et al., 2024): N = northern clade; S = southern clade.

PHYLOGENETIC ANALYSES

Our concatenated multigene dataset (appendix 1) comprises 2306 bp with 18.2% missing data. The gene-partitioning scheme identified by IQ-TREE required separate substitution models for CYTB (best-fitting model: GTR+I+G), IRBP (best-fitting model: K2P+I), and FGB (best-fitting model: HKY+G). Maximum-likelihood analysis of these data resulted in a fully resolved tree (fig. 9), most aspects of which were also recovered by our Bayesian analysis. Unfortunately, however, most nodes are not strongly supported. Separate analyses of our mitochondrial and nuclear sequences (not shown) suggest that there is no strong phylogenetic signal in our nuclear data, so the low support for most nodes is unlikely to be the result of mitochondrial-nuclear conflicts.

Despite generally low nodal support, there are several noteworthy features of this topology. One is a basal dichotomy between a moderately supported clade that we propose to call the Trinitatis Group (*Oecomys catherinae* + *O. matogrossensis* + *O. flavicans* + *O. trinitatis* + *O. rex*) on the one hand and a clade with strong Bayesian support that includes all the remaining species of *Oecomys* on the other. Within the latter clade, several multispecies groups received strong support from one or both analyses, including those we propose to call the Rutilus Group (*O. rutilus* + *O. hiceae* + *O. trabeatus*), the Bicolor Group (*O. bicolor* + *O. cleberi* + *O. nanus* + *O. jamari* + *O. phaeotis*), and the Mamorae Group (*O. franciscorum* + *O. mamorae*). Within the Rutilus Group, a sister-group relationship between *O. rutilus* and *O. hiceae* is strongly supported by our Bayesian results. Within the Bicolor Group, *O. bicolor* + *O. cleberi* form a strongly supported clade, but relationships among *O. jamari*, *O. nanus*, and *O. phaeotis* are not convincingly resolved. Within the Trinitatis Group, *O. catherinae* + *O. matogrossensis* is a consistently strongly supported clade, and *O. trinitatis* + *O. flavicans* is another.

The remaining relationships recovered in these analyses receive no more than moderate (70%–94%) bootstrap support, but several observations seem appropriate. First, there is obviously no support for a close relationship between *O. paricola* and *O. hiceae* despite the fact that specimens of *O. hiceae* were previously identified as *O. paricola* (see above). Second, although

FIG. 8. Primary lowland rainforest along the Río Jesusito, Darién province, Panama, type locality of *Oecomys trabeatus*. Photographed by Thomas Barbour in 1922. (Image W745151 from the photographic archives of the Ernst Mayr Library at the Museum of Comparative Zoology, Harvard University.)

O. trabeatus has long been considered a junior synonym of *O. bicolor*, these taxa do not appear to be closely related either. Third, there is no support for a clade consisting of *O. concolor*, *O. mamorae*, and *O. sydandersoni*, three species that share a derived carotid morphology previously interpreted as evidence for a close relationship (Carleton et al., 2009). Lastly, we note that the wide separation between *O. galvez* and *O. trinitatis* is consistent with their recent recognition as separate species (Voss et al., 2024).

DISCUSSION

Although stronger support for many nodes in our phylogenetic reconstruction is much to be desired, the results in hand seem sufficient to support the recognition of at least three species groups, and we tentatively recognize two others in the following accounts. In effect, these proposed groups are hypotheses of monophyly that merit testing by future analyses based on more extensive genetic and phenotypic data.

Three Strongly Supported Groups

Rutilus Group: This robustly supported but previously unsuspected clade includes *Oecomys hiceae*, *O. rutilus*, and *O. trabeatus*. These species share phenotypic traits that are widely

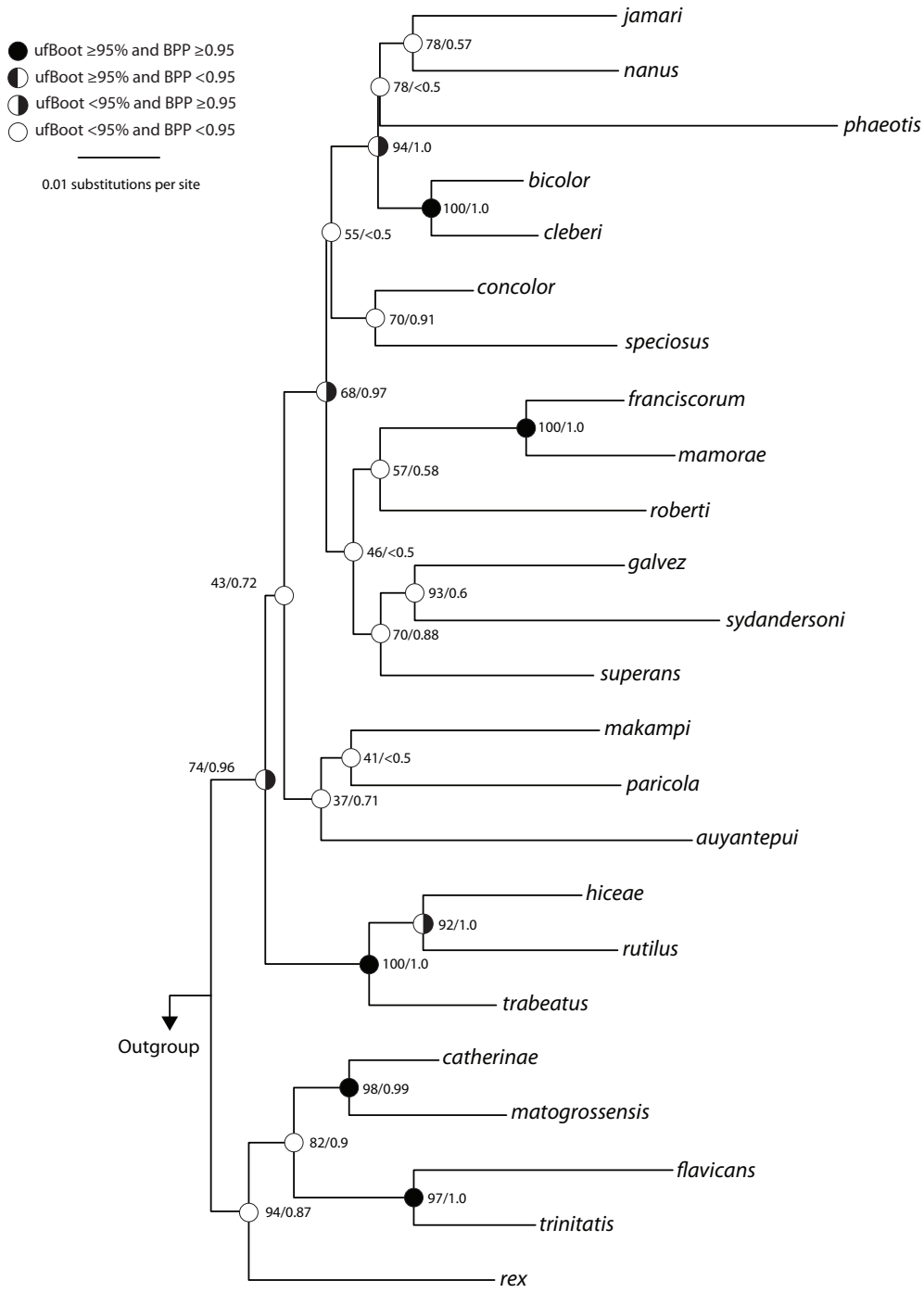

FIG. 9. Maximum-likelihood (ML) phylogeny of *Oecomys* based on concatenated sequences of one mitochondrial and two nuclear genes. Nodal support statistics include ultrafast bootstrap values (ufBoot, expressed as percentages) from the ML analysis and posterior probabilities (expressed as decimal fractions, BPP) from a Bayesian analysis of the same data.

exhibited by other congeners (e.g., small size, penciled tails, shallow zygomatic notches, pattern 1 carotid circulation, alisphenoid struts), so none is diagnostic of group membership. Distributional and morphological comparisons among member taxa are summarized in table 9. *Oecomys rutilus*, which is endemic to the Guiana Region (northeastern Amazonia), is by far the smallest member this group, with a mean value for crown length of the upper molars (LM) that is seven standard deviations smaller than the mean value of this dimension for *O. hiceae*, its sister species. *Oecomys hiceae* is the only group member that often has gray-based ventral fur between the fore- and hind legs, whereas the ventral fur of the others is immaculately self-white from chin to anus. *Oecomys hiceae* is also the only species with an accessory labial root on M1, a structure not seen in the other species. By contrast, *O. trabeatus* lacks unique morphological traits, but it is the only group member that occurs west of the Andes. Unfortunately, karyotypic information is only available for *O. rutilus* (table 10), so chromosomal similarities and differences among these species cannot be assessed. Mitochondrial DNA sequence comparisons will be provided in a subsequent report (Voss et al., MS), but we note that the branch lengths separating group members on our tree are within the range of branch lengths observed among currently recognized species in other groups.

Bicolor Group: This clade includes *Oecomys bicolor*, *O. cleberi*, *O. jamari*, *O. nanus*, and *O. phaeotis*. Most of these are small species (mean LM <4 mm) with self-white ventral fur, shallow zygomatic notches, pattern 1 carotid circulation, large parietal extensions onto the lateral braincase, and (insofar as known) high diploid numbers ($2n \geq 80$). None of these traits, however, is uniquely diagnostic, because *O. rutilus* and *O. trabeatus* (members of the Rutilus Group; see above) are similar in all listed morphological features, and at least two species currently unassigned to group (*O. roberti* and *O. superans*) have equally high diploid numbers (table 10). Additionally, the specimens that we refer to *O. phaeotis* are substantially larger than other group members (LM = 4.2–4.7 mm) and sometimes have indistinctly gray-based ventral fur. Therefore, phenotypic and karyotypic support for this group is equivocal.

It seems likely that additional diversity within the Bicolor Group will be recognized with future taxonomic research. Even disembarrassed of *Oecomys trabeatus*, *O. bicolor* (sensu Carleton and Musser, 2015) includes several other nominal taxa as junior synonyms—*benevolens* Thomas, 1901; *rosilla* Thomas, 1904; *nitedulus* Thomas, 1910; *milleri* J.A. Allen, 1916; *florenciae* J.A. Allen, 1916; *phelpsi* Tate, 1939—and some of these may yet prove to be valid species. The failure of several molecular studies to resolve *O. bicolor* and *O. cleberi* as reciprocally monophyletic taxa (Suárez-Villota et al., 2018; Saldanha et al., 2023) is another relevant issue. Lastly, analyses of cytochrome *b* sequence data (e.g., Voss et al., 2024: fig. 27) suggest the existence of yet unnamed western Amazonian forms that are closely related to *O. nanus*.

The Bicolor Group occupies most of the forested cis-Andean lowlands of tropical South America with the notable exception of the Atlantic Forest. *Oecomys bicolor*, *O. jamari*, and *O. nanus* are all Amazonian species (Saldanha et al., 2023; Voss et al., 2024; this report),[9] as are

[9] The taxonomic status of specimens from northern Venezuela previously identified as *Oecomys bicolor* (e.g., by Handley, 1976; Carleton and Musser, 2015) is unclear. The few examples we examined have longer dorsal fur, longer ungual tufts, longer tails, and longer caudal pencils than typical *O. bicolor*, and we assume they represent a distinct species.

TABLE 9. Geographic and morphological comparisons among species of the Rutilus Group of *Oecomys* as recognized in this report.

	O. hiceae	*O. rutilus*	*O. trabeatus*
Distribution	NW Amazonia	Guiana Region	TransAndean
Hind foot (HF)	24 ± 1 mm	21 ± 1 mm	23 ± 1 mm
Upper molars (LM)	4.0 ± 0.1 mm	3.3 ± 0.1	3.9 ± 0.1 mm
Ventral fur coloration	usually gray-based	always self-white	always self-white
M1 accessory root	present	absent	absent

the aforementioned cytochrome *b* haplogroups related to *O. nanus*; by contrast, *O. cleberi* is a Cerrado species (Brandão et al., 2024), and *O. phaeotis* occurs in montane forest along the eastern Andes of southern Peru and northern Bolivia. Examples of sympatry between group members have been reported from northern Peru and western Brazil (where *O. bicolor* and *O. nanus* co-occur; Voss et al., 2024), whereas *O. cleberi* and *O. jamari* have been collected sympatrically in Rondônia (Saldanha et al., 2023), and the existence of dissimilar coat-color phenotypes among specimens identified as *O. bicolor* from southern Venezuela (Ochoa et al., 2009) suggest that group members might be sympatric elsewhere.

Mamorae Group: A sister-group relationship between *Oecomys mamorae* and *O. franciscorum* is noncontroversial because these species closely resemble one another morphologically, and they have adjacent geographic distributions in eastern Bolivia, Paraguay, southern Brazil, and northern Argentina (Pardiñas et al., 2016; Suárez-Villota et al., 2018).

Two Additional Groups

Concolor Group: Nodal statistics for this group of two species (*Oecomys concolor* and *O. speciosus*) are less than the threshold values for statistical significance, but additional sequence data could provide more compelling evidence of a close relationship. Interestingly, although these species are strikingly dissimilar phenotypically—notably in carotid arterial morphology (Carleton and Musser, 2015)—they have contiguous or narrowly overlapping geographic ranges. Whereas *Oecomys concolor* occupies the Rio Negro and upper Orinoco basins, *O. speciosus* occurs in landscapes drained by the middle-to-lower Orinoco, along the Caribbean coastal watersheds of Colombia and Venezuela, and on the island of Trinidad (Carleton and Musser, 2015: maps 207, 215). Specimens of both species have been collected sympatrically in the Llanos (at Hato Cariben [6.55°N, 67.22°S]; Handley, 1976).

Trinitatis Group: This basal clade of five species (*Oecomys catherinae*, *O. flavicans*, *O. matogrossensis*, *O. rex*, and *O. trinitatis*) receives only moderate support from our analyses, but a similar result obtained by Gomes et al. (2016: fig. 6) from analyses of COI sequence data suggests that stronger molecular support will be forthcoming from larger datasets.[10] Based on our examination of voucher material and other representative specimens, members

[10] Gomes et al.'s (2016: fig. 6) COI gene tree included a clade of five terminals that they identified as *Oecomys rex*. However, our examination of voucher material suggests that only three of these (INPA 5049, HQ919650,

TABLE 10. Karyotypes of *Oecomys* species, arranged by hypothetical group membership.

	2*n*	FN	Reference
Bicolor Group			
O. bicolor	80	140	Patton et al. (2000)
O. cleberi	80	124–134	Suárez-Villota et al. (2018)
O. jamari	—	—	
O. nanus	86	98	Patton et al. (2000)[a]
Concolor Group			
O. concolor[b]	—	—	
O. speciosus	68	—	This report[c]
Mamorae Group			
O. franciscorum	72	90	Suárez-Villota et al. (2018)
O. mamorae	—	—	
Rutilus Group			
O. hiceae	—	—	
O. rutilus	54	90	Gomes et al. (2016), this report[d]
O. trabeatus	—	—	
Trinitatis Group			
O. catherinae	60–62	62	Suárez-Villota et al. (2018)
O. flavicans	—	—	
O. matogrossensis	54	54	Saldanha and Rossi (2021)
O. trinitatis[e]	—	—	
O. rex	62	86	Lira (2012)
Unassigned species			
O. auyantepui	64–72	80–114	Lira (2012), Gomes et al. (2016), Silva et al. (2022)
O. galvez	58	96	Patton et al. (2000)[a]
O. makampi	—	—	
O. paricola	68–70	72–76	Suárez-Villota et al. (2018)
O. roberti	80–82	106–114	Suárez-Villota et al. (2018)
O. superans	80	108	Patton et al. (2000)
O. sydandersoni	—	—	

[a] See Voss et al. (2024).
[b] Sensu stricto (Carleton and Musser, 2015). Karyotypes previously associated with this name (e.g., by Gardner and Patton, 1976; Baker et al., 1983) were obtained from misidentified specimens.
[c] Based on a single karyotyped female (USNM 448583) from Apure, Venezuela.
[d] A single karyotyped female (MHNLS 7841) from Bolívar, Venezuela, has the same diploid number as the Brazilian specimens reported by Gomes et al. (2016).
[e] Sensu stricto (see text).

of this group share the following traits, which we tentatively regard as diagnostic: large size (mean adult weight >40 g); long (≥10 mm on average) and distinctively soft dorsal fur; gray-based ventral fur (except on the chin and throat of some species); tails that lack a terminal pencil of distinctly longer hairs; hind feet with dense ungual tufts of silvery hairs that are usually longer than the claws on digits II–V; deep zygomatic notches (relative to notch development in other groups); complete carotid circulations (pattern 1 of Voss, 1988); and strongly opisthodont upper incisors. Although morphological character polarities have yet to be convincingly established within *Oecomys*, this suite of shared traits tends to support the notion that members of the Trinitatis Group are closely related, as does the rather narrow range of diploid and fundamental numbers exhibited by group members with known karyotypes ($2n$ = 54–62; table 10).

Oecomys rex is easily distinguished morphologically from other members of the Trinitatis Group by (inter alia) its prominent supraorbital crests, large postorbital processes, broad petrosal-squamosal overlap, and laterally occluded postglenoid foramen (Carleton and Musser, 2015). Other members of this group are distinguished from one another by much subtler differences, and their morphological recognition is correspondingly problematic. For example, although Carleton and Musser (2015) recognized *O. trinitatis* and *O. catherinae* as distinct species, most of the specimens they referred to *O. trinitatis* from south of the Amazon in Brazil correspond to *O. catherinae* sensu Suárez-Villota et al. (2018).[11] Following Voss et al., 2024), we restrict *O. trinitatis* to the morphologically homogeneous populations that occur on the islands of Trinidad and Tobago and on the immediately adjacent Venezuelan mainland; in addition to the nominotypical form, *O. trinitatis* in this strict sense includes *fulviventer* J.A. Allen, 1899; *palmarius* J.A. Allen, 1899; and *splendens* Hayman, 1938. By contrast, the taxonomic status of other nominal taxa that Carleton and Musser (2015) treated as junior synonyms of *O. trinitatis* (including *frontalis* Goldman, 1912; *helvolus* J.A. Allen, 1913; *klagesi* J.A. Allen, 1904; *osgoodi* Thomas, 1924; *subluteus* Thomas, 1898; *tectus* Thomas, 1901; and *vicencianus* J.A. Allen, 1913) remains to be determined, but at least some of them seem likely to represent valid species.

The Trinitatis Group is widespread, occurring from eastern Costa Rica (Hall, 1980: map 366) eastward and southward throughout Panama and much of tropical and subtropical cis-Andean South America to southeastern Brazil. To our knowledge, species of this group have not been collected in sympatry. Curiously, members of this group are unknown from much of the western Amazonian lowlands (e.g., in the well-sampled Yavarí-Ucayali interfluve of Loreto department, Peru; Voss et al., 2024).

---

and JQ601068) are *O. rex*, whereas the other two (JF491659, JF491660) represent *O. trinitatis* sensu Carleton and Musser (2015).

[11] Including specimens subsequently described as *Oecomys matogrossensis* by Saldanha and Rossi (2021). However, the specimens that Patton et al. (2000) reported as *O. trinitatis* from the Rio Juruá were reidentified by Voss et al. (2024: 75–82) as *O. galvez*.

Other Relationships

A clade that includes all the species of *Oecomys* except members of the Trinitatis Group is strongly supported by our Bayesian analysis, but it receives only moderate maximum-likelihood support. This clade includes seven species that do not belong to any of the groups proposed herein. Of these, three large western Amazonian species—*O. galvez*, *O. sydandersoni*, and *O. superans*—form a clade with moderate support from both analyses, whereas three others—*O. auyantepui*, *O. makampi*, and *O. paricola*—form a clade with only weak support. Lastly, we recovered *O. roberti* as the weakly supported sister taxon of the Mamorae Group. Although we treat all these species as monotypic for the purpose of phylogeny reconstruction, some have been hypothesized to conceal cryptic taxonomic diversity.

Several authors have recognized a group of species (or putative species) closely related to *Oecomys roberti*, but, in our opinion, recognition of a Roberti Group is premature. As recognized by Carleton and Musser (2015), *O. roberti* ranges throughout Amazonia and includes two nominal taxa as junior synonyms: *guianae* Thomas, 1910, and *tapajinus* Thomas, 1909. Analyses of cytochrome *b* sequence data (Patton et al., 2000; Rocha et al., 2018; Suárez-Villota et al., 2018; Voss et al., 2024) have consistently documented deep phylogeographic structure in this widespread species, but neither phenotypic nor karyotypic differences have been convincingly correlated with mtDNA divergence, and the taxonomic application of junior synonyms is unclear (Voss et al., 2024: 82–84). Pending a critical taxonomic revision of this complex, it seems prudent to recognize only a single species.

Oecomys paricola (in the strict sense of this report) and *O. auyantepui* are other species that are thought to conceal cryptic taxonomic diversity (Suárez-Villota et al., 2018; Silva et al., 2020, 2022), but there seems to be no compelling morphological evidence of multiple species corresponding to current usage of either name. In assessing the likelihood of cryptic taxa in these and other cases, alternative hypotheses such as chromosomal polymorphism (versus karyotypic speciation) and geographically discontinuous sampling (versus allopatric speciation) merit careful evaluation. Above all, it must be recalled that sequence-based "species delimitation" methods, especially those based exclusively on mitochondrial genes, are prone to many sources of bias and misinterpretation, all of which suggest taxonomic caution in the absence of supporting evidence from other sources (Carstens et al., 2013; Dávalos and Russell, 2014; Sukumaran and Knowles, 2017; Mason et al., 2020; Wüster et al., 2024).

Concluding Remarks

Although morphological characters are useful for taxonomic diagnoses, they sometimes provide misleading evidence of phylogenetic relationships in *Oecomys*. One obvious example of flawed taxonomic inference from morphological similarity is the set of taxa that Hershkovitz (1960) synonymized with *O. bicolor* (then including *O. rutilus* and *O. trabeatus*) based on their small size and self-white ventral pelage. Another is the set of species (*O. concolor*, *O. mamorae*, and *O. sydandersoni*) that Carleton et al. (2009) hypothesized to be closely related based on their shared carotid morphology. A third example (if confirmed by future research) might be

the close relationship between *O. concolor* and *O. speciosus*, previously unsuspected due to their widely dissimilar phenotypes.

Of course, it is possible that our phylogenetic results are misleading, or that we have placed undue confidence in nodal support for some recovered groups. Sequence data from additional mitochondrial genes, and filling gaps in the dataset already in hand, are twin priorities for future research. Another priority is continuing revisionary efforts to distinguish valid species among allegedly synonymous nominal taxa (e.g., the putative synonyms of *O. trinitatis*), as well as fresh collections from mammalogically sparsely explored regions, and renewed study of long-ignored specimens that are already in museums. The picture that is slowly emerging from research to date is that *Oecomys* is much more speciose than previously suspected.

ACKNOWLEDGMENTS

We thank the curators and support staffs of museums that hosted our visits or loaned specimens, tissues, or other material for this report, including Ned Gilmore (ANSP); Roberto Portela and Paula Jenkins (BMNH); Adam Ferguson, Larry Heaney, Bruce Patterson, and John Phelps (FMNH); Jocelyn Colella (KU); Steve Cardiff and Jake Esselstyne (LSUMZ); Mark Omura (MCZ); Joe Cook and Jon Dunnum (MSB); Victor Pacheco (MUSM); Robert Bradley and Heath Garner (TTU); Cody Thompson (UMMZ); and Missy Hawkins, Darrin Lunde, and Megan Viera (USNM).

Michelle Koo (at the MVZ) and Ned Gilmore (ANSP) kindly provided copies of O.P. Pearson's 1938 field notes from Panama, which were helpful in reconstructing his collecting itinerary. We are grateful to Yuri Leite and Léo Gomes for tracking down the voucher specimen corresponding to the GenBank sequences of *Oecomys catherinae* that we downloaded from GenBank. Lisa Bradley generously allowed us to re-use a habitat photo previously published in the TTU Special Publications series. Patricia J. Wynne drew figures 1, 3, and 5 with her characteristic elegance, and she composed figures 4 and 7 from photographs taken by Nicole Wong. For assistance with laboratory work at Siena College, we thank Thomas Anderson, Amy Perry, and Kate Putnum. We thank Kristen Choffee for sequencing at ROM. Lastly, we thank Marcus Brandão, Sharon Jansa, and Marcelo Weksler for reading our submitted draft and making helpful suggestions that enhanced the final version of this report; however, they are not to blame for any inaccuracies or omissions that might remain in our text, tables, appendices, or figures.

REFERENCES

Allen, G.M., and T. Barbour. 1923. Mammals from Darien. Bulletin of the Museum of Comparative Zoology 45: 259–274.

Ammerman, L.K., D.N. Lee, and T.M. Tipps. 2012. First molecular phylogenetic insights into the evolution of free-tailed bats in the subfamily Molossinae (Molossidae, Chiroptera). Journal of Mammalogy 93: 12–28.

Baker, R.J., B.F. Koop, and M.W. Haiduk. 1983. Resolving systematic relationships with G-bands: a study of five genera of South American cricetine rodents. Systematic Zoology 32: 403–416.

Bangs, O., and T. Barbour. 1922. Birds from Darien. Bulletin of the Museum of Comparative Zoology 65: 191–229.

Barbour, T. 1944. Naturalist at large. Boston: Little, Brown, and Company.

Bass, M.S., et al. 2010. Global conservation significance of Ecuador's Yasuní National Park. PLoS ONE 5 (1): e8767.

Brandão, M.V., G.S.T. Garbino, G.C. Rezende, S.F. Tenório, and S.F. Reis. 2024. Taxonomic and natural history notes on *Oecomys cleberi* (Rodentia: Cricetidae) and first records in the Atlantic Forest, Brazil. Studies on Neotropical Fauna and Environment 59: 59–73.

Cabrera, A. 1961. Catálogo de los mamíferos de América del Sur. Revista del Museo Argentino de Ciencias Naturales "Bernardino Rivadavia" (Ciencias Zoológicas) 4 (2): 309–732.

Calle-Rendón, B.R., M. Peck, S.E. Bennett, C. Morelos-Juarez, and F. Alfonso. 2016. Comparison of forest regeneration in two sites with different primate abundances in northwestern Ecuador. Revista de Biología Tropical 64: 493–506.

Carleton, M.D., and G.G. Musser. 2015. Genus *Oecomys* Thomas, 1906. *In* J.L. Patton, U.F.J. Pardiñas, and G. D'Elía (editors), Mammals of South America, vol. 2: rodents: 393–417. Chicago: University of Chicago Press.

Carleton, M.D., L.H. Emmons, and G.G. Musser. 2009. A new species of the rodent genus *Oecomys* (Cricetidae: Sigmodontinae: Oryzomyini) from eastern Bolivia, with emended definitions of *O. concolor* (Wagner), and *O. mamorae* (Thomas). American Museum Novitates 3661: 1–32.

Carstens, B.C., T.A. Pelletier, N.M. Reid, and J.D. Satler. 2013. How to fail at species delimitation. Molecular Ecology 22: 4369–4383.

Croat, T.B. 1978. Flora of Barro Colorado Island. Stanford: Stanford University Press.

Dávalos, L.M., and A.L. Russell. 2014. Sex-biased dispersal produces high error rates in mitochondrial distance-based and tree-based species delimitation. Journal of Mammalogy 95: 781–791.

Delacre, M., D. Lakens, and C. Leys. 2017. Why psychologists should by default use Welch's *t*-test instead of Student's *t*-test. International Review of Social Psychology 30: 92–101.

Díaz, M.M. 2020. Lista comentada de los pequeños roedores de Iquitos y sus alrededores. Boletim do Museu Paraense Emílio Goeldi Ciências Naturais Belém 15: 727–766.

Dodson, C.H., and A.H. Gentry. 1978. Flora of the Río Palenque Science Center, Los Ríos, Ecuador. Selbyana (Journal of the Marie Selby Botanical Gardens) 4: i–xxx, 1–628.

Duellman, W.E., and J.R. Mendelson III. 1995. Amphibians and reptiles from northern Departamento Loreto, Peru: taxonomy and biogeography. University of Kansas Science Bulletin 55: 329–376.

Fairchild, G.B., and C.O. Handley Jr. 1966. Gazetteer of collecting localities in Panama. *In* R.L. Wenzel and V.J. Tipton (editors), Ectoparasites of Panama: 9–22 + folding map.

Gardner, A.L., and J.L. Patton. 1976. Karyotypic variation in oryzomyine rodents (Cricetinae) with comments on chromosomal evolution in the Neotropical cricetine complex. Occasional Papers of the Museum of Zoology of Louisiana State University 49: 1–48.

Giarla, T.C., and R.S. Voss. 2020. DNA sequence data from the holotype of *Marmosa elegans coquimbensis* Tate, 1931 (Mammalia: Didelphidae) resolve its disputed relationships. American Museum Novitates 3946: 1–8.

Goldman, E.A. 1933. A new climbing mouse from Panama. Journal of the Washington Academy of Sciences 23: 525–526.

Gomes,, R.G., Jr., et al. 2016. Intense genomic reorganization in the genus *Oecomys* (Rodentia, Sigmodontinae): comparison between DNA barcoding and mapping of repetitive elements in three species of the Brazilian Amazon. Comparative Cytogenetics 10: 401–426.

Hall, E.R. 1962. Collecting and preparing study specimens of vertebrates. Miscellaneous Publications, University of Kansas Museum of Natural History 30: 1–46.

Hall, E.R. 1980. The mammals of North America, 2 vols. New York: John Wiley & Sons.

Handley, C.O. Jr. 1976. Mammals of the Smithsonian Venezuelan Project. Brigham Young University Science Bulletin, Biological Series 20 (5): 1–89 + map.

Hershkovitz, P. 1960. Mammals of northern Colombia, preliminary report no. 8. Arboreal rice rats, a systematic revision of the subgenus *Oecomys*, genus *Oryzomys*. Proceedings of the United States National Museum 110: 513–568 + 12 pls.

Hice, C.L., and P.M. Velazco. 2012. The non-volant mammals of the Reserva Nacional Allpahuayo-Mishana, Loreto, Peru. Special Publications of the Museum of Texas Tech University 60: [i, ii], 1–135.

Hice, C.L., P.M. Velazco, and M. Willig. 2004. Bats of the Reserva Nacional Allpahuayo-Mishana, northeastern Peru, with notes on community structure. Acta Chiropterologica 6: 319–334.

Katoh, K., and D.M. Standley. 2013. MAFFT multiple sequence alignment software version 7: improvements in performance and usability. Molecular Biology and Evolution 30 (4): 772–780.

Leigh, E.G. Jr, A.S. Rand, and D.M. Windsor (eds.). 1996. The ecology of a tropical forest, 2nd ed. Washington DC: Smithsonian Institution Press.

Lim, B.K., M.D. Engstrom, J.W. Bickham, and J.C. Patton. 2008. Molecular phylogeny of New World sheath-tailed bats (Emballonuridae: Diclidurini) based on loci from the four genetic transmission systems in mammals. Biological Journal of the Linnean Society 93: 189–209.

Lira, T. de. 2012. Citogenética clássica e molecular de alguns representantes da tribo Oryzomyini (Rodentia, Cricetidae) da Amazônia Central. Postgraduate thesis, Instituto Nacional de Pesquisas da Amazônia (Manaus).

Mason, N.A., N.K. Fletcher, B.A. Gill, W.C. Funk, and K.R. Zamudio. 2020. Coalescent-based species delimitation is sensitive to geographic sampling and isolation by distance. Systematics and Biodiversity 18: 269–280.

Minh, B.Q., M.A.T. Nguyen, and A. von Haesler. 2013. Ultrafast approximation for phylogenetic bootstrap. Molecular Biology and Evolution 30 (5): 1188–1195.

Minh, B.Q., et al. 2020. IQ-TREE 2: new models and efficient methods for phylogenetic inference in the genomic era. Molecular Biology and Evolution 37 (5): 1530–1534.

Musser, G.G., and M.D. Carleton. 1993. Family Muridae. *In* D.E. Wilson and D.M. Reeder (editors), Mammal species of the world, 2nd ed.: 501–755. Washington DC: Smithsonian Institution Press.

Ochoa G., J., F. García, S. Caura, and J. Sánchez H. 2009. Mamíferos de la cuenca del río Caura, Venezuela: listado taxonómico y distribución conocida. Memoria de la Fundación La Salle de Ciencias Naturales 170: 5–80.

Pardiñas, U.F.J., P. Teta, J. Salazar-Bravo, P. Myers, and C.A. Galliari. 2016. A new species of arboreal rat, genus *Oecomys* (Rodentia, Cricetidae) from Chaco. Journal of Mammalogy 97: 1177–1196.

Patton, J.L. 1967. Chromosome studies of certain pocket mice, genus *Perognathus* (Rodentia: Heteromyidae). Journal of Mammalogy 48: 27–37.

Patton, J.L., and M.N.F. da Silva. 1995. A review of the spiny mouse genus *Scolomys* (Rodentia: Muridae: Sigmodontinae) with the description of a new species from the western Amazon of Brazil. Proceedings of the Biological Society of Washington 108: 319–337.

Patton, J.L., M.N.F. da Silva, and J.R. Malcolm. 2000. Mammals of the Rio Juruá and the evolutionary and ecological diversification of Amazonia. Bulletin of the American Museum of Natural History 244: 1–306.

Paynter, R.A. Jr. 1993. Ornithological gazetteer of Ecuador, 2nd ed. Cambridge, MA: Museum of Comparative Zoology.

Percequillo, A.R., M. Weksler, and L.P. Costa. 2011. A new genus and species of rodent from the Brazilian Atlantic Forest (Rodentia: Cricetidae: Sigmodontinae: Oryzomyini), with comments on oryzomyine biogeography. Zoological Journal of the Linnean Society 161: 357–390.

Pitman, N.C.A. 2000. A large-scale inventory of two Amazonian tree communities. Ph.D. dissertation, Duke University.

Prance, G.T. 1979. Notes on the vegetation of Amazonia III. The terminology of Amazonian forest types subject to inundation. Brittonia 31: 26–38.

Rambaut, A., A.J. Drummond, D. Xie, G. Baele, and M.A. Suchard. 2018. Posterior summarization in Bayesian phylogenetics using Tracer 1.7. Systematic Biology 67 (5): 901–904.

Rocha, R.G., et al. 2011. Small mammals of the mid-Araguaia River in central Brazil, with the description of a new species of climbing rat. Zootaxa 2789: 1–34.

Rocha, R.G., C. Fonseca, Z. Zhou, Y.L.R. Leite, and L.P. Costa. 2012. Taxonomic and conservation status of the elusive *Oecomys cleberi* (Rodentia, Sigmodontinae) from central Brazil. Mammalian Biology 77: 414–419.

Rocha, R.G. et al. 2018. Cryptic diversity in the *Oecomys roberti* complex: revalidation of *Oecomys tapajinus* (Rodentia: Cricetidae). Journal of Mammalogy 99: 174–186.

Ronquist, F., et al. 2012. MrBayes 3.2: efficient Bayesian phylogenetic inference and model choice across a large model space. Systematic Biology 61 (3): 539–542.

Rosa, C.C. et al. 2012. Genetic and morphological variability in South American rodent *Oecomys* (Sigmodontinae, Rodentia): evidence for a complex of species. Journal of Genetics 91: 265–277.

Saldanha, J., and R.V. Rossi. 2021. Integrative analysis supports a new species of the *Oecomys catherinae* complex (Rodentia, Cricetidae) from Amazonia. Journal of Mammalogy 102: 69–89.

Saldanha, J., et al. 2023. Unveiling hidden diversity of *Oecomys* (Rodentia: Cricetidae) from Brazilian central Amazonia: description of a new species and new lineages. Systematics and Biodiversity 21 (1): 2259037.

Siegel, D.C., and S.L. Olson. 2008. The birds of the republic of Panama. Part 5. Ornithological gazetteer and bibliography. Shipman, VA: Buteo Books.

Silva, W.O. da, et al. 2020. Karyotypic divergence reveals that diversity in the *Oecomys paricola* complex (Rodentia, Sigmodontinae) from eastern Amazonia is higher than previously thought. PLoS ONE 15(10): e0241495.

Silva, W.O. da, et al. 2022. The emergence of a new sex-system (XX/XY_1Y_2) suggests a species complex in the "monotypic" rodent *Oecomys auyantepui* (Rodentia, Sigmodontinae). Scientific Reports 12: 8690.

Steppan, S.J., and J.J. Schenk. 2017. Muroid rodent phylogenetics: 900-species tree reveals increasing diversification rates. PLoS ONE 12 (8): e0183070.

Suárez-Villota, E.Y., A.P. Carmignotto, M.V. Brandão, A.R. Percequillo, and M.J.J. de Silva. 2018. Systematics of the genus *Oecomys* (Sigmodontinae: Oryzomyini): molecular phylogenetic, cytogenetic, and morphological approaches reveal cryptic species. Zoological Journal of the Linnean Society 184: 182–210.

Sukumaran, J., and L.L. Knowles. 2017. Multispecies coalescence delimits structure, not species. Proceedings of the National Academy of Sciences of the United States of America 114: 1607–1612.

Thomas, O. 1900. Descriptions of new Neotropical mammals. Annals and Magazine of Natural History (ser. 7) 5: 269–274.

Thomas, O. 1906. Notes on South American rodents. Annals and Magazine of Natural History (ser. 7) 18: 442–448.

Valencia, R., et al. 2004. Tree species distributions and local habitat variation in the Amazon: large forest plot in eastern Ecuador. Journal of Ecology 92: 214–229.

Vásquez M., R., and Oliver L. Phillips. 2000. Allpahuayo: floristics, structure, and dynamics of a high-diversity forest in Amazonian Peru. Annals of the Missouri Botanical Garden 87: 499–527.

Vormisto, J., O.L. Phillips, K. Ruokolainen, H. Tuomisto, and R. Vásquez. 2000. A comparison of fine-scale distribution patterns of four plant groups in an Amazonian rainforest. Ecography 23: 349–359.

Voss, R.S. 1988. Systematics and ecology of ichthyomyine rodents (Muroidea): patterns of morphological evolution in a small adaptive radiation. Bulletin of the American Museum of Natural History 188 (2): 259–493.

Voss, R.S., and A.V. Linzey. 1981. Comparative gross morphology of male accessory glands among Neotropical Muridae (Mammalia: Rodentia) with comments on systematic implications. Miscellaneous Publications of the Museum of Zoology, University of Michigan 159: i–iv, 1–41.

Voss, R.S., D.W. Fleck, and T.C. Giarla. 2024. Mammalian diversity and Matses ethnomammalogy in Amazonian Peru. Part 5. Rodents. Bulletin of the American Museum of Natural History 466: 1–179.

Voss, R.S., T.C. Giarla, B.K. Lim, and M.D. Engstrom. MS. An introduction to *Oecomys* (Rodentia: Cricetidae) from the Guiana Region, with biogeographic comments.

Wallace, A.R. 1854. On the monkeys of the Amazon. Proceedings of the Zoological Society of London 1852: 107–110.

Weksler, M. 2003. Phylogeny of Neotropical oryzomyine rodents (Muridae: Sigmodontinae) based on the nuclear IRBP exon. Molecular Phylogenetics and Evolution 29: 331–349.

Weksler, M. 2006. Phylogenetic relationships of oryzomyine rodents (Muroidea: Sigmodontinae): separate and combined analyses of morphological and molecular data. Bulletin of the American Museum of Natural History 296: 1–149.

Wüster, W. et al. 2024. How not to describe a species: lessons from a tangle of anacondas. Zoological Journal of the Linnean Society 201: zlae099 (AOP).

APPENDIX 1

Multigene Dataset for Analyses of *Oecomys* Phylogeny

Species	Voucher[a]	Field No.[b]	Locality[c]	CYTB	IRBP	FGB	Source
auyantepui	ROM 115156	F46766	GU: Cuyuni-Mazaruni	PV641719	PV641730	PV641741	this study
bicolor	ROM 104505*	F37351	EC: Orellana	PV641720	PV641731	PV641742	this study
catherinae	UFMG [uncat][d]	LGV 75[d]	BR: Minas Gerais	MG323772	MG323693	MG323774	Suárez-Villota et al. (2018)
cleberi	MN 71672	APC 562	BR: Goiás	MG323746	MG323667	MG323830	Suárez-Villota et al. (2018)
concolor	USNM 406013*		VE: Amazonas	PV641721	—	—	this study
flavicans	AMNH 21327*		VE: Mérida	PV641722	—	—	this study
franciscorum	MZUSP 35540	PNPA 300	BR: Mato Grosso	MG323716	MG323637	MG323786	Suárez-Villota et al. (2018)
galvez	AMNH 276720*	MVC 363	PE: Loreto	PP001549	PV641732	PV641743	Voss et al. (2024), this study
hiceae	TTU 98907*	TK73722	PE: Loreto	PP001564	PV641733	PV641744	Voss et al. (2024), this study
jamari	UFROM 624	RMFJMDF 012	BR: Rondônia	OR339672	—	OR339663	Saldanha et al. (2023)
makampi	MUSM 15335*	DWF 730	PE: Loreto	PP001554	PV641734	PV641745	Voss et al. (2024), this study
mamorae	MSB 68481	NK 25352	BO: Beni	KT737227	—	—	Pardiñas et al. (2016)
matogrossensis	MZUSP 35535	APC 243	BR: Mato Grosso	MG323759	MG323680	MG323841	Suárez-Villota et al. (2018)
nanus	AMNH 276713*	JAA 864	PE: Loreto	PP001558	PV641735	PV641746	Voss et al. (2024), this study
paricola	MZUSP 30332	UUPI 005	BR: Piauí	MG323705	MG323626	MG323797	Suárez-Villota et al. (2018)
phaeotis	FMNH 170599*	BDP 3858	PE: Cusco	PP001611	—	PV641747	Voss et al. (2024), this study
rex	ROM 121070*	F53783	SU: Sipaliwini	PV641723	PV641736	PV641748	this study
roberti	MZUSP 35547	APM 751	BR: Mato Grosso	MG323722	MG323643	MG323809	Suárez-Villota et al. (2018)
rutilus	ROM 111580*	F44709	GU: Potaro-Siparuni	PV641724	PV641737	PV641749	this study
speciosus	CM 78755*	MWH 319	VE: Bolívar	PV641725	PV641738	PV641750	this study
superans	ROM 106144*	F40402	EC: Orellana	PV641726	PV641739	PV641751	this study
sydandersoni	USNM 588189[d]	LHE 1407	BO: Santa Cruz	KT737235	—	—	Pardiñas et al. (2016)
trabeatus	MSB 222115*	NK185763	PA: Colón	PV641727	PV641740	PV641752	this study
trinitatis	AMNH 186736*		T&T: Trinidad	PV641729	—	—	this study

[a] See Materials and Methods for institutional abbreviations. Asterisks identify specimens examined by R.S.V. to confirm identifications.

[b] Sometimes used as tissue identifiers; not listed for sequences obtained from historical material.

[c] Country and next-largest administrative unit (state/department/province/region/island). Abbreviations: BO, Bolivia; BR, Brazil; EC, Ecuador; GU, Guyana; PA, Panama; PE, Peru; SU, Suriname; T&T, Trinidad and Tobago; VE, Venezuela.

[d] The GenBank records for MG323772, MG323693, and MG323774 give the "voucher number" as CIT 2096, which is the same as the "field number" listed in Suárez-Villota et al.'s (2018) supplementary information; the latter document also states that the voucher is an uncataloged specimen at UFES. However, neither the tissue sample nor the voucher specimen are at UFES. According to Y.L.R. Leite (in litt., 7 March 2025), CIT 2096 is the number assigned to a tissue sample in Yatiyo Yonenaga-Yassuda's lab at USP; apparently, the voucher is a still uncataloged specimen at UFMG with field number LGV 75.

APPENDIX 2

Cytochrome *b* Sequences for Genetic Distance Comparisons between *Oecomys hiceae* and *O. paricola*

Species[a]	Voucher[b]	Field #	Locality[c]	GenBank#	Source
hiceae	ROM 104473*	F37313	EC: Orellana, 38 km S Pompeya Sur	PP001562	Voss et al. (2024)
hiceae	ROM 106213	F40426	EC: Orellana, 38 km S Pompeya Sur	PP001563	Voss et al. (2024)
hiceae	TTU 98907*	TK73722	PE: Loreto 25 km S. Iquitos	PP001564	Voss et al. (2024)
hiceae	TTU 101252*	TK75156	PE: Loreto 25 km S. Iquitos	PP001565	Voss et al. (2024)
hiceae	KU 158190*	NW 827	PE: Loreto, San Jacinto	PP001566	Voss et al. (2024)
hiceae	MUSM [uncat]	PSV 241	PE: Loreto, Llanchama	MG824902	MUSM project[d]
hiceae	MUSM 44977	VPT 4439	PE: Loreto, Llanchama	MG824908	MUSM project[d]
hiceae	MUSM 44978	KPB 1666	PE: Loreto, Llanchama	MG824891	MUSM project[d]
hiceae	MUSM 44980*	KPB 1619	PE: Loreto, Llanchama	MG824911	MUSM project[d]
hiceae	MUSM 45736	PSV 73	PE: Loreto, Llanchama	MG824897	MUSM project[d]
paricola E	MZUSP [uncat]	ESTR123	BR: Maranhão, Carolina	MG323704	Suárez-Villota et al. (2018)
paricola E		BAR017	BR: Pará, Barcarena	JF759676	Rosa et al. (2012)
paricola E		BAR013	BR: Pará, Barcarena	JF759675	Rosa et al. (2012)
paricola E		BAR023	BR: Pará, Barcarena	JF759677	Rosa et al. (2012)
paricola E		BAR029	BR: Pará, Barcarena	JF759678	Rosa et al. (2012)
paricola E	MPEG 38659		BR: Pará, Belém	JF759679	Rosa et al. (2012)
paricola E	MPEG 38664		BR: Pará, Belém	JF759680	Rosa et al. (2012)
paricola E	MPEG 39699		BR: Pará, Belém	JF759681	Rosa et al. (2012)
paricola E	MPEG 39701		BR: Pará, Belém	JF759682	Rosa et al. (2012)
paricola E	MPEG 39705		BR: Pará, Belém	JF759683	Rosa et al. (2012)
paricola E	MPEG 39708		BR: Pará, Belém	JF759684	Rosa et al. (2012)
paricola E	MZUSP [uncat]	UU43	BR: Piauí, Estação Ecológico de Uruçuí-Una	MG323707	Suárez-Villota et al. (2018)
paricola E	MZUSP 30332	UUPI005	BR: Piauí, Estação Ecológico de Uruçuí-Una	MG323705	Suárez-Villota et al. (2018)
paricola E	MZUSP 30340	UUPI457	BR: Piauí, Estação Ecológico de Uruçuí-Una	MG323706	Suárez-Villota et al. (2018)
paricola E	MZUSP 35552	APC1240	BR: Tocantins, Estação Ecológico Serra Geral Tocantins	MG323702	Suárez-Villota et al. (2018)
paricola E	MZUSP 35553	APC1260	BR: Tocantins, Estação Ecológico Serra Geral Tocantins	MG323703	Suárez-Villota et al. (2018)
paricola E	MZUSP 35551	APC1532	BR: Tocantins, Estação Ecológico Serra Geral Tocantins	MG323701	Suárez-Villota et al. (2018)

APPENDIX 2 *continued*

Species[a]	Voucher[b]	Field #	Locality[c]	GenBank#	Source
paricola E	UFES 1368		BR: Tocantins, Pium	HM594590	Rocha et al. (2011)
paricola E	UFES 1438		BR: Tocantins, Pium	HM594589	Rocha et al. (2011)
paricola N	MPEG 40842		BR: Pará, Marajó Island	JF759668	Rosa et al. (2012)
paricola N	MPEG 40843		BR: Pará, Marajó Island	JF759669	Rosa et al. (2012)
paricola N	MPEG 40844		BR: Pará, Marajó Island	JF759671	Rosa et al. (2012)
paricola N	MPEG 40845		BR: Pará, Marajó Island	JF759670	Rosa et al. (2012)
paricola N	MPEG 40848		BR: Pará, Marajó Island	JF759672	Rosa et al. (2012)
paricola N	MPEG 40849		BR: Pará, Marajó Island	JF759673	Rosa et al. (2012)
paricola N	MPEG 40851		BR: Pará, Marajó Island	JF759674	Rosa et al. (2012)
paricola W	MZUSP 29525	M97023	BR: Mato Grosso, Cláudia	MG323713	Suárez-Villota et al. (2018)
paricola W	MZUSP 29527	M97073	BR: Mato Grosso, Cláudia	MG323711	Suárez-Villota et al. (2018)
paricola W	MZUSP [uncat]	M97109	BR: Mato Grosso, Cláudia	MG323708	Suárez-Villota et al. (2018)
paricola W	MZUSP 29530	M97141	BR: Mato Grosso, Cláudia	MG323709	Suárez-Villota et al. (2018)
paricola W	MZUSP [uncat]	M97148	BR: Mato Grosso, Cláudia	MG323710	Suárez-Villota et al. (2018)
paricola W	MZUSP 35545	M976296	BR: Mato Grosso, Cláudia	MG323712	Suárez-Villota et al. (2018)
paricola W	MVZ 197507		BR: Mato Grosso, Reserva Ecológica Cristalino	HM594592	Rocha et al. (2011)
paricola W	MVZ 197508		BR: Mato Grosso, Reserva Ecológica Cristalino	HM594593	Rocha et al. (2011)
paricola W	UFMG 2841		BR: Mato Grosso, Reserva Ecológica Cristalino	HM594591	Rocha et al. (2011)

[a] Including putative taxa recognized by Suárez-Villota et al. (2018) in the *Oecomys paricola* complex: E, eastern clade; N, northern clade; W, western clade.
[b] See Materials and Methods for institutional abbreviations. Asterisks identify specimens examined by R.S.V. to confirm identifications.
[c] Country abbreviations: BR, Brazil; EC, Ecuador; PE, Peru.
[d] "Caracterización molecular de roedores reservorios de enfermedades emergentes en la región amazónica y modelamiento de su distribución para la identificación de áreas de alto riesgo: caso hantavirus."

APPENDIX 3

Cytochrome *B* Sequences for Genetic Distance Comparisons between *Oecomys bicolor* and *O. trabeatus*

Species[a]	Voucher[b]	Field #	Locality[c]	GenBank#	Source
bicolor (N)	MVZ 200956*	JUR 566	BR: Amazonas, Colocação Vira-Volta	PP001501	Voss et al. (2024)
bicolor (N)	ROM 105519*	F37752	EC: Orellana, 35 km S Pompeya Sur	PP001502	Voss et al. (2024)
bicolor (N)	ROM 105597*	F37840	EC: Orellana, 35 km S Pompeya Sur	PP001503	Voss et al. (2024)
bicolor (N)	ROM 105660*	F37905	EC: Orellana, 35 km S Pompeya Sur	PP001504	Voss et al. (2024)
bicolor (N)	ROM 104505*	F37351	EC: Orellana, 42 km S Pompeya Sur	PP001505	Voss et al. (2024)
bicolor (N)	ROM 118911*	F41922	EC: Orellana, 42 km S Pompeya Sur	PP001506	Voss et al. (2024)
bicolor (N)	TTU 84901*	TK104129	EC: Pastaza, 5 km E Puyo	PP001507	Voss et al. (2024)
bicolor (N)	TTU 85228*	TK104456	EC: Pastaza, 5 km E Puyo	PP001508	Voss et al. (2024)
bicolor (N)	MVZ 154988*	JLP 7341	PE: Amazonas, Huampami	PP001509	Voss et al. (2024)
bicolor (N)	MVZ 154990*	JLP 7354	PE: Amazonas, Huampami	PP001510	Voss et al. (2024)
bicolor (N)	MVZ 154991*	JLP 7360	PE: Amazonas, Huampami	PP001511	Voss et al. (2024)
bicolor (N)	MVZ 154992*	JLP 7373	PE: Amazonas, Huampami	PP001512	Voss et al. (2024)
bicolor (N)	MVZ 154997*	JLP 7618	PE: Amazonas, Huampami	PP001513	Voss et al. (2024)
bicolor (N)	MVZ 154999*	JLP 7645	PE: Amazonas, Huampami	PP001514	Voss et al. (2024)
bicolor (N)	MVZ 155001*	JLP 7690	PE: Amazonas, Huampami	PP001515	Voss et al. (2024)
bicolor (N)	TTU 100834*	TK73027	PE: Loreto, 25 km S Iquitos	PP001516	Voss et al. (2024)
bicolor (N)	TTU 98621*	TK73046	PE: Loreto, 25 km S Iquitos	PP001517	Voss et al. (2024)
bicolor (N)	TTU 98829*	TK73532	PE: Loreto, 25 km S Iquitos	PP001518	Voss et al. (2024)
bicolor (N)	MUSM 17571*	LAC 392	PE: Loreto, Collpa Salvador	MG824904	MUSM project[d]
bicolor (N)	MUSM 17638	LAC 459	PE: Loreto, Collpa Salvador	MG824906	MUSM project[d]
bicolor (N)	MUSM 16000*	JAA 238	PE: Loreto, Jenaro Herrera	MG824899	MUSM project[d]
bicolor (N)	MUSM [uncat]	PSV 232	PE: Loreto, Llanchama	MG824903	MUSM project[d]
bicolor (N)	MUSM [uncat]	PSV 214	PE: Loreto, Llanchama	MG824901	MUSM project[d]
bicolor (N)	MUSM 44979	KPB 1573	PE: Loreto, Nina Rumi	MG824890	MUSM project[d]
bicolor (N)	MUSM 45737*	VPT 4486	PE: Loreto, Nina Rumi	MG824892	MUSM project[d]
bicolor (N)	MUSM 45738*	VPT 4495	PE: Loreto, Nina Rumi	MG824894	MUSM project[d]
bicolor (N)	MUSM 45739*	PSV 27	PE: Loreto, Nina Rumi	MG824895	MUSM project[d]
bicolor (N)	MUSM 45740*	VPT 4474	PE: Loreto, Nina Rumi	MG824909	MUSM project[d]
bicolor (N)	MUSM 45741*	VPT 4494	PE: Loreto, Nina Rumi	MG824910	MUSM project[d]
bicolor (N)	MUSM 45742*	VPT 4491	PE: Loreto, Nina Rumi	MG824893	MUSM project[d]
bicolor (N)	MUSM 45743*	PSV 31	PE: Loreto, Nina Rumi	MG824896	MUSM project[d]
bicolor (N)	AMNH 272674*	RSV 2046	PE: Loreto, Nuevo San Juan	PP001519	Voss et al. (2024)

APPENDIX 3 *continued*

Species[a]	Voucher[b]	Field #	Locality[c]	GenBank#	Source
bicolor (N)	MUSM 13315*	RSV 2070	PE: Loreto, Nuevo San Juan	PP001520	Voss et al. (2024)
bicolor (N)	MUSM 13316*	RSV 2099	PE: Loreto, Nuevo San Juan	PP001521	Voss et al. (2024)
bicolor (N)	MUSM 43188*	MDO 656	PE: Loreto, Pachacutec	MG824905	MUSM project[d]
bicolor (N)	FMNH 203674*	PMV 2371	PE: San Martín, Tingana	PP001522	Voss et al. (2024)
bicolor (S)	MVZ 200958*	MNFS 1260	BR: Acre, Igarapé Porongaba	PP001523	Voss et al. (2024)
bicolor (S)	MVZ 200959*	MNFS 1261	BR: Acre, Igarapé Porongaba	PP001524	Voss et al. (2024)
bicolor (S)	MVZ 200963*	MNFS 1679	BR: Acre, Nova Vida	PP001525	Voss et al. (2024)
bicolor (S)	MVZ 200882*	MNFS 1333	BR: Acre, opposite Igarapé Porongaba	PP001526	Voss et al. (2024)
bicolor (S)	MVZ 200962*	MNFS 1499	BR: Acre, Sobral	PP001527	Voss et al. (2024)
bicolor (S)	MVZ 200884*	JLP 15777	BR: Amazonas, Barro Vermelho	PP001528	Voss et al. (2024)
bicolor (S)	MVZ 200964*	MNFS 749	BR: Amazonas, Barro Vermelho	PP001529	Voss et al. (2024)
bicolor (S)	MVZ 200966*	JLP 15414	BR: Amazonas, Nova Empresa	PP001530	Voss et al. (2024)
bicolor (S)	MVZ 200967*	JLP 15433	BR: Amazonas, Nova Empresa	PP001531	Voss et al. (2024)
bicolor (S)	MVZ 200897*	MNFS 651	BR: Amazonas, Sacado	PP001532	Voss et al. (2024)
bicolor (S)	MVZ 200971*	MNFS 652	BR: Amazonas, Sacado	PP001533	Voss et al. (2024)
bicolor (S)	KU 144302*	CAS 686	PE: Madre de Dios, Cusco Amazónico	PP001534	Voss et al. (2024)
bicolor (S)	KU 144304*	CAS 701	PE: Madre de Dios, Cusco Amazónico	PP001535	Voss et al. (2024)
bicolor (S)	KU 144305*	CAS 721	PE: Madre de Dios, Cusco Amazónico	PP001536	Voss et al. (2024)
bicolor (S)	KU 144314*	NW 609	PE: Madre de Dios, Cusco Amazónico	PP001537	Voss et al. (2024)
bicolor (S)	KU 144322*	RMT 3926	PE: Madre de Dios, Cusco Amazónico	PP001538	Voss et al. (2024)
bicolor (S)	KU 144325*	RMT 3934	PE: Madre de Dios, Cusco Amazónico	PP001539	Voss et al. (2024)
bicolor (S)	KU 144327*	NW 692	PE: Madre de Dios, Cusco Amazónico	PP001540	Voss et al. (2024)
trabeatus	MSB 222115*	NK185763	PA: Colón, Parque Nacional Soberanía	PV641727	this study
trabeatus	MSB 222113*	NK185764	PA: Colón, Parque Nacional Soberanía	PV641728	this study

[a] Including putative taxa recognized by Voss et al. (2024) in the *Oecomys bicolor* complex: N, northern clade; S, southern clade.

[b] See Materials and Methods for institutional abbreviations. Asterisks identify specimens examined by R.S.V. to confirm identifications.

[c] Country abbreviations: BR, Brazil; EC, Ecuador; PA, Panama; PE, Peru.

[d] "Caracterización molecular de roedores reservorios de enfermedades emergentes en la región amazónica y modelamiento de su distribución para la identificación de áreas de alto riesgo: caso hantavirus."

APPENDIX 4

Gazetteer of Collection Localities

This gazetteer includes all the localities from which we personally examined specimens of *Oecomys hiceae* and *O. trabeatus*. Italicized geographic names are those of departments, provinces, or states; boldface identifies locality names as they appear in the text of this report. The name(s) of species collected at each locality is separated from the locality name and geographic data by a colon, followed by the name(s) of the collector(s) and date(s) of collection (if known) in parentheses. Numbers identify locality symbols plotted on our map (fig. 3).

ECUADOR

1. *Esmeraldas*, **Pambilar** (ca. 0.62°N, 79.17°W, 200–800 m; Calle-Rendón et al., 2016): *Oecomys trabeatus* (G. Fleming, 21 August–18 September 1900). The above coordinates are for a protected area that is now known as the Refugio de Vida Silvestre El Pambilar; we assume that this is, or is close to, an hacienda or village named Pambilar in Fleming's day.
2. *Esmeraldas*, **San Javier** (1.07°N, 78.78°W, ca 100 m; Paynter, 1993): *Oecomys trabeatus* (G. Fleming and R. Miketta, 28 July 1900).
3. *Imbabura*, **Paramba** (= Hacienda Paramba at 0.82°N, 78.35°W, 777 m; Paynter, 1993): *Oecomys trabeatus* (R. Miketta, 11 May 1899). Thomas (1900) gave the elevation of Paramba as 1100 m, but Hacienda Paramba is at 777 m according to Paynter (1993), who said it is (or was) on the south bank of the Río Mira.
4. *Los Ríos*, **58 km SW Santo Domingo de los Colorados**, (ca. 0.61°S, 79.51°W, 240 m; see below): *Oecomys trabeatus* (G. Hammond, 1 August 1914). The collector's verbatim locality (on the skin tag of BMNH 15.1.1.56) reads "36 M S by W of Santo Domingo." The same label also gives the elevation as 800 ft (244 m) and the coordinates as 0°35′S, 79°10′W. According to Paynter (1993), Hammond worked at Santo Domingo de los Colorados (0.25°S, 79.15°W) in July 1914 and at Quevedo (1.03°S, 79.48°W) in August, so this locality must have been somewhere along the road between those towns. Santo Domingo is in Pichincha province, but 36 miles (58 kilometers) along the road to Quevedo would securely place this locality in Los Ríos. Our estimated coordinates suggest a locality about 40 km west of that indicated by Hammond's.
5. *Orellana*, **Parque Nacional Yasuní**, Onkone Gare (0.66°S, 76.45°W), 38 km S Pompeya Sur: *Oecomys hiceae* (ROM team, 13 May 1995).

PANAMA

6. *Colón*, **Camp Piña** (9.28°N, 79.98°W, 50 m; Siegel and Olson, 2008): *Oecomys trabeatus* (C.O. Handley Jr., 28 August 1956).
7. *Colón*, **Parque Nacional Soberanía** (9.17°N, 79.69°W [ca. 200 m; Siegel and Olson, 2008]): *Oecomys trabeatus* (Hantavirus survey team, 8 February 2010). This locality is only about 18 km from Barro Colorado Island (9.15°N, 79.85°W), the type locality of *Oecomys endersi*.
8. *Darién*, **Guayabo** (= Ensenada del Jayabo at 7.42°N, 78.05°W, near sea level; Siegel and Olson, 2008): *Oecomys trabeatus* (O.P. Pearson, 24 May–13 June 1938). Pearson's field notes

(archived at ANSP and MVZ) say that he camped on the beach at Guayabo, a remote bay on the Pacific coast.

9. *Darién*, **Pelisa** (not located; 500 ft [152 m]): *Oecomys trabeatus* (O.P. Pearson, 4 February 1938). Fairchild and Handley (1966) thought this locality might be on the Río Pavarando (ca. 7.82°N, 78.07°W; Siegel and Olson, 2008), which arises in the Serranía del Sapo, but Pearson's fieldnotes (archived at ANSP and MVZ) say that Pelisa was only a little over two hours by trail from El Tigre ("a location, not a town"), which he reached via El Real (8.13°N, 77.72°W) and Boca de Cupé (8.05°N, 77.58°W) on his way to Cana (ca. 7.75°N, 77.70°W); this itinerary would put Pelisa somewhere in the valley of the Río Tuira, which drains the eastern slopes of the Serranía de Pirre. According to the same source, Cana was about 10 hours by trail with pack horses from Pelisa; assuming that two km/hour is a reasonable rate of travel with laden horses, we mapped this locality about 20 km north of Cana, or about 28 km north of the Colombian border.
10. *Darién*, **Río Jesusito** (ca. 8.03°N, 78.30°W; Siegel and Olson, 2008): *Oecomys trabeatus* (T. Barbour and W.S. Brooks, 10 April 1922). According to Bangs and Barbour (1922: 193), "Jesusito refers to camps at several points in the lowland forest on the Río Jesusito, which rises in the Sapo Mountains [Serranía del Sapo]." The identification of the photograph in our text (fig. 8) is based on the captioned plate facing page 76 in Barbour's autobiography (Barbour, 1944).[1]
11. *Darién*, **Tacarcuna Village** (8.08°N, 77.28°W, ca. 700 m; Siegel and Olson, 2008): *Oecomys trabeatus* (R. Hinds, P. Galindo, and G. Barrett; 16 July 1963).
12. *Panamá*, **Cerro Azul** (9.17°N, 79.40°W, ca. 600 m; Siegel and Olson, 2008): *Oecomys trabeatus* (C.O. Handley Jr., 9 June 1957 and 2–4 February 1958).
13. *San Blas*, Armila, **Quebrada Venado** (8.67°N, 77.48°W, near sea level; Siegel and Olson, 2008): *Oecomys trabeatus* (C.O. Handley Jr. and F. M. Greenwell, 23 February–24 March 1963).

PERU

14. *Loreto*, **El Triunfo** (4.16°S, 73.48°W; Díaz, 2020), Km 49.5 carretera Iquitos-Nauta, 120 m: *Oecomys hiceae* (C.L. Hice, 11 May 2002).
15. *Loreto*, **Estación Biológica Allpahuayo** (3.94°S, 73.60°W; Díaz, 2020), 25 km S Iquitos: *Oecomys hiceae* (C.L. Hice, 28 December 1997, 14 April–8 November 1998). Most skin tags of specimens collected at this locality (including the tag tied to the holotype of *O. hiceae*) include the phrase "25 km S Iquitos," but (as noted above), Hice and Velazco (2012: 3) stated that the biological station is 28 km southwest of Iquitos on the road to Nauta.
16. *Loreto*, **La Habana** (4.19°S, 73.48°W), Km 52 on Iquitos-Nauta highway: *Oecomys hiceae* (C.L. Hice, 9 September 2002).
17. *Loreto*, **Llanchama** (3.87°S, 73.40°W; Díaz, 2020), 114 m: *Oecomys hiceae* (K. Pino, 23 September 2015).
18. *Loreto*, **San Jacinto** (2.32°S, 75.87°W; Duellman and Mendelson, 1995): *Oecomys hiceae* (N. Woodman, 6 July 1993).

[1] Available online (https://archive.org/details/naturalistatlarg00barb).